Mohit Narwal

Selective Inhibition of Human Tankyrases

Mohit Narwal

Mohit Narwal was born on January 20, 1984 in Nahan, H.P., India. He did his Bachelor and Master of Science in Biotechnology from Panjab University and IIT Roorkee, respectively in India. This PhD thesis work has taken place under the supervision of Dr. Lari Lehtiö at Pharmaceutical Sciences, Åbo Akademi University and Faculty of Biochemistry and Molecular Medicine, University of Oulu during 2009-2014.

Selective Inhibition
of Human Tankyrases

Mohit Narwal

**Pharmaceutical Sciences
Department of Biosciences
Åbo Akademi University
Turku, Finland**

2014

Supervisor   **Dr. Lari Lehtiö**

Docent
Biocenter Oulu
Faculty of Biochemistry and Molecular Medicine
University of Oulu
Finland

Reviewer   **Dr. Tommi Kajander**

Docent,
Institute of Biotechnology
University of Helsinki
Finland

And

Dr. Jens Preben Morth

Center for Molecular Medicine
University of Oslo
Norway

Opponent   **Dr. Herwig Schüler**

PI Structural Biochemistry
Department of Medical Biochemistry and
Biophysics
Karolinska Institutet
Sweden

Cover: Crystal structure of tankyrase 2 in complex with IWR-1
My photo: Picture by Bhargav Prabhakar

Table of Contents

Original Publications

The thesis is based on the following publications, mentioned in the text by the Roman numerals **I-V**. Publications are reprinted with the permissions from the publishers.

  I.   M. Narwal, A. Fallarero, P.M. Vuorela, L. Lehtiö, (2012) Homogeneous screening assay for human tankyrase. *J Biomol Screen*. **17**(5):593-604.

  II.   M. Narwal, H. Venkannagari, L. Lehtiö, (2012) Structural basis of selective inhibition of human tankyrases. *J Med Chem*. **55**(3):1360-1367.

  III.   M. Narwal, T. Haikarainen, A. Fallarero, P.M. Vuorela, L. Lehtiö, (2013) Screening and structural analysis of flavones inhibiting tankyrases. *J Med Chem*. **56**(9):3507-3517.

  IV.   M. Narwal, J. Koivunen, T. Haikarainen, E. Obaji, O. E. Legala, H. Venkannagari, P. Joensuu, T. Pihlajaniemi, Lehtiö L, (2013) Discovery of tankyrase inhibiting flavones with increased potency. *J Med Chem.* **55**(20):7880-7889.

  V.   T. Haikarainen*, M. Narwal*, P. Joensuu, Lehtiö L, (2013) Evaluation and structural basis for the inhibition of tankyrases by PARP inhibitors. *ACS Med Chem. Lett.* **5**(1):18-22.

*equal contribution

Contributions of the author

Studies were designed and manuscripts were written together with the supervisor. All the co-authors contributed to the final manuscripts.

I. Protein expression and purification, assay development, compounds screening and measurement of potencies were done by the author. Statistical analysis was done together with the help of Dr. Adyary Fallerero.

II. Protein expression and purification, and protein X-ray crystallographic studies were performed by the author.

III. Protein expression and purification, assay development, screening of the compounds, and potency measurements were done by the author. Protein X-ray crystallographic studies were performed together with Dr. Teemu Haikarainen.

IV. Screening of the compounds, potency measurements and protein X-ray crystallographic studies were done by the author.

V. Screening of the compounds and potency measurements were performed by the author.

Additional publications not included in thesis

S.C. Vilchez Larrea, T. Haikarainen, M. Narwal, M. Schlesinger, H. Venkannagari, M.M. Flawiá, S.H. Villamil, L. Lehtiö, (2012) Inhibition of poly(ADP-ribose) polymerase interferes with Trypanosoma cruzi infection and proliferation of the parasite. *PLoS One*. **7**(9):e46063.

T. Haikarainen, H., M. Narwal, E. Obaji, H.W. Lee, Y. Nkizinkiko, L. Lehtiö, (2013) Structural basis and selectivity of tankyrase inhibition by a Wnt signaling inhibitor WIKI4. *PLoS One*. **8**(6):e65404

T. Haikarainen, J. Koivunen, M. Narwal, H. Venkannagari, E. Obaji, P. Joensuu, T. Pihlajaniemi, L. Lehtiö, (2013) para-Substituted 2-Phenyl-3,4-dihydroquinazolin-4-ones As Potent and Selective Tankyrase Inhibitors. *ChemMedChem*. **8**(12):1978-1985.

Acknowledgements

telling me when I did something stupid, you were and are there for everything, no bargaining or explanations needed.

All along the biggest support system I had and have is my family. Thank you Mumma and Papa, my lovely niece (Harveen), my brother (Rohit), my sister (Shiwani) and her family, for their endless love and support over the years. Their unconditional support has been a true inspiration during my PhD studies and in many other fronts. Mere words are not enough to express the gratitude I feel for my family. I cherish our times together.

Finally, I would like to thank everybody who was important for the successful realization of this thesis, as well as expressing my apology if I missed on someone. I take along my most cherished memories as I embark on next phase of my life.

Abstract

Tankyrases belong to the Diphtheria toxin-like ADP-ribosyltransferase (ARTD) enzyme superfamily, also known as poly(ADP-ribose) polymerases (PARPs). They catalyze a covalent post-translational modification reaction where they transfer ADP-ribose units from NAD^+ to target proteins. Tankyrases are involved in many cellular processes and their roles in telomere homeostasis, Wnt signaling and in several diseases including cancers have made them interesting drug targets. In this thesis project, selective inhibition of human tankyrases was studied.

A homogeneous fluorescence-based assay was developed to screen the compound libraries. The assay is inexpensive, operationally easy, and performs well according to the statistical analysis. Assay suitability was confirmed by screening a natural product library. Flavone was identified as the most potent inhibitor in the library and this motivated us to screen a larger flavonoid library. Results showed that flavones were indeed the best inhibitor of tankyrases among flavonoids. To further study the structure-activity relationship, a small library of flavones containing single substitution was screened and potency measurements allowed us to generate structure-activity relationship. Compounds containing substitutions at 4′-position were more potent in comparison to other substitutions, and importantly, hydrophobic groups improved isoenzyme selectivity as well as the potency. A flavone derivative containing a hydrophobic isopropyl group (compound **22**), displayed 6 nM potency against TNKS1, excellent isoenzyme selectivity and Wnt signaling inhibition. Protein interactions with compounds were studied by solving complex crystal structures of the compounds with TNKS2 catalytic domain. A novel tankyrase inhibitor (IWR-1) was also crystallized in complex with TNKS2 catalytic domain. The crystal structure of TNKS2 in complex with IWR-1 showed that the compound binds to adenosine site and it was the first known ARTD inhibitor of this kind.

To date, there is no structural information available about the substrate binding with any of the ARTD family members; therefore NAD^+ was soaked with TNKS2 catalytic domain crystals. However, analysis of crystal structure showed that NAD^+ was hydrolyzed to nicotinamide. Also, a co-crystal structure of NAD^+ mimic compound, EB-47, was solved which was used to deduce some insights about the substrate interactions with the enzyme.

Like EB-47, other ARTD1 inhibitors were also shown to inhibit tankyrases. It indicated that selectivity of the ARTD1 inhibitors should be considered as some of the effects in cells could come from tankyrase inhibition.

In conclusion, the study provides novel information on tankyrase inhibition and presents new insight into the selectivity and potency of compounds.

Abbreviations

3-AB	3-aminobenzamide
3BP2	c-Abl Src homology 3 domain-binding protein-2
ADP	adenosine diphosphate
APC	adenomatous polyposis coli
AR	automodification region
ARC	ankyrin repeat cluster
ARH	ADP-ribosyl hydrolase-3
ARTD	diphtheria toxin-like ADP-ribosyltransferase
AXIN	axis inhibition protein
$BioNAD^+$	biotinylated nicotinamide adenine dinucleotide
BLZF1	basic leucine zipper nuclear factor 1
BRCA	breast cancer type 1 susceptibility protein
BRCT	breast cancer susceptibility protein C-terminus motif
CACNA 1S	alpha 1S subunit of the voltage-dependent L-type calcium channel
CASC3	cancer susceptibility candidate 3
CG-NAP	centrosome and Golgi localized protein kinase N-associated protein
CK1	cyclin-dependent kinase
CPAP	centrosomal P4.1-associated protein
DBD	dna binding domain
EBNA	epstein-barr nuclear region
EC_{50}	half maximal effective concentration
EGFR	epidermal growth factor receptor
FIH	factor inhibiting hypoxia inducible factor
FNBP1/FBP17	formin-binding protein 1
GDP	glucose-6-phosphate
GF	gel filteration
GLUT4	glucose transporter type 4
GMD	GDP-mannose 4,6–dehydratase
GRB14	growth factor receptor-bound protein 14
GSK	glycogen synthase kinase
HD	helical domain
HOXB2	homeobox protein

HPS	polymeric repeats of histidine, proline and serine
HSV	herpes simplex virus
IC_{50}	half maximal inhibitory concentration
ICP0	HSV-infected cell polypeptide
IPTG	isopropyl-β-D-thiogalactoside
IRAP	insulin-regulated aminopeptidase
KIF3A	kinesin motor protein
MAPK	mitogen-activated protein kinase
MCL-1	myeloid cell leukemia
MDR	multi drug resistance
MEK	mitogen activated kinase
MVP-ID	major vault protein particle interacting domain
NAD^+	nicotinamide adenine dinucleotide
NI	nicotinamide binding site
Ni-affinity	Nickle affinity
NuMA	nuclear mitotic apparatus protein
PAR	poly(ADP-ribose)
PARG	poly(ADP-ribose) glycohydrolase
PARP	poly(ADP-ribose) polymerase
PI31	proteasome inhibitor 31
PLK1	polo-like kinase 1
POT-1	protection of telomeres 1
PP12C	polymorphic variant of the protein phosphatase 1 regulated subunit 12 C
RD	regulatory domain
RNF146	RING finger protein 146
RNP	ribonucleoprotein
SAM	sterile alpha motif
SAF	scaffold-associated factor
SAP	scaffold-associated protein
SD	standard deviation
SDS-PAGE	sodium dodecyl sulfate polyacrylamide gel electrophoresis
TAB182	182- kDa tankyrase binding protein
TAB1BP1	tax1-binding protein 1
TCEP	tris (2-carboxyethyl) phosphine

TCF	T Cell Factor
TIN2	TRF interacting protein
TNKS	tankyrase
TPP1	tripeptidyl-peptidase 1
TRF	telomere repeat factor
UPS	ubiquitin-proteasome system
USP25	ubiquitin-specific protease 25
VIT	vault protein inter-α-trypsin
vWA	von Willebrand type A
WGR	tryptophan, glycine, arginine rich
WWE	tryptophan, and glutamate rich

1 Review of the literature

1.1 Introduction

Nicotinamide adenine dinucleotide (NAD^+) is a coenzyme involved in several redox reactions in the living cells (Belenky *et al*, 2007). NAD^+ binds to the proteins through special types of protein folds. The most established of them is Rossmann fold, which was first found in the nucleotide binding proteins such as dehydrogenase (Rossmann *et al*, 1974). It is a protein structural motif consisting of six parallel beta strands linked to two pairs of alpha helices. It binds to NAD^+ through a pair of Rossmann folds because one fold can bind to only one nucleotide moiety. In addition, domain containing Rossmann fold also binds to NAD^+ of three other known classes of proteins. These include ADP-ribosyltransferases, ADP ribosyl cyclases and sirtuins (Belenky *et al*, 2007; Koch-Nolte *et al*, 2009). This thesis focuses on human ADP-ribosyltransferases (ARTDs) (EC 2.4.2.30), previously known as poly(ADP-ribosyl) polymerases (PARPs). ARTDs were first described in 1960s and since then they have been implicated in wide range of cellular processes (Chambon *et al*, 1963). ARTDs catalyze poly(ADP)ribosylation (PARsylation) reaction and modify proteins that mediate DNA-damage repair, cell signaling, energy metabolism and gene transcription (Hassa & Hottiger, 2008).

To date, seventeen members of this enzyme superfamily have been identified and some of them have been characterized. ARTD family members cleave NAD^+ to nicotinamide and ADP-ribose, and attach the ADP-ribose moieties onto target proteins (heteromodification) or on themselves (automodification) reviewed in (Hottiger *et al*, 2010) (**Fig. 1**). In order to discover the acceptor sites for ADP-ribosylations, a mutant of ARTD1 capable of catalyzing only mono-ADP-ribosylation was used and ribosylated product was separated using HPLC. Mass spectrometric analysis of digested ribosylated product with trypsin revealed that glutamate and aspartate residues act as acceptor sites for ADP-ribosylation reaction (Tao *et al*, 2009). In another study, chemical linkage stability studies utilizing the automodification reaction capacity of PARP1/ARTD1 showed that lysines also act as the acceptor sites for ADP-ribosylation (Altmeyer *et al*, 2009a).

It was noticed that some of the family members were not able to catalyze the polymerization reaction but function as mono ADP-ribosyl transferases (Kleine *et al*, 2008; Otto *et al*, 2005). This led to a new proposed nomenclature of PARPs as Diphtheria toxin like ADP-ribosyltransferases (ARTDs) (Hottiger *et al*, 2010).
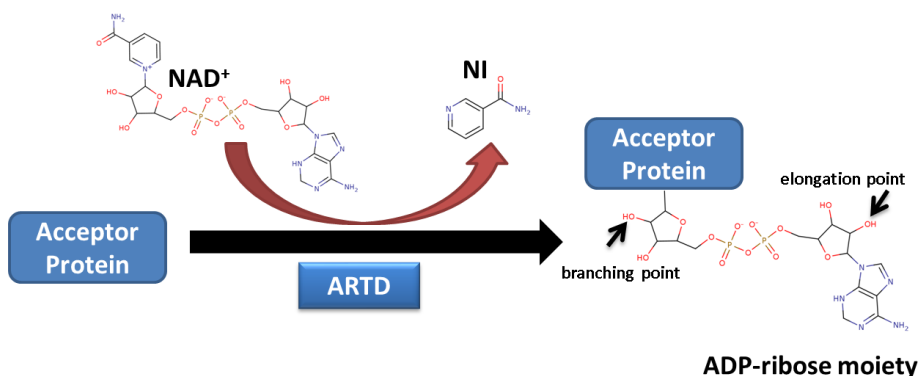
Figure 1. ARTDs hydrolyze the substrate NAD$^+$ and catalyze the covalent modification of the acceptor protein by adding the ADP-ribose units onto mainly glutamate, aspartate or lysine residues. Elongation and branching points are also indicated.

ARTD1/PARP1 and ARTD2/PARP2 are able to synthesize linear or branched ADP-ribose polymers and the length of the polymers could reach 200 units *in vitro* and *in vivo* (Alvarez-Gonzalez & Jacobson, 1987; Juarez-Salinas *et al*, 1983, 1982; Kanai *et al*, 1982; Miwa *et al*, 1981). Catalytic activity of ARTD3/PARP3 and ARTD4/PARP4 is not well-studied. However, ARTD1, ARTD2 and ARTD3 interacts with DNA and co-operates with the catalytic domain, and their activity is DNA-dependent (Amé *et al*, 1999; Boehler *et al*, 2011; Langelier *et al*, 2010). Tankyrases (PARP5A/TNKS1/ARTD5 and PARP5B/TNKS2/ARTD6) are known to form linear oligomers, only up to an approximate length of 20 subunits and no branching has been observed yet (Rippmann *et al*, 2002). ARTD7, ARTD8 and ARTD10 are characterized as mono ADP-ribosyltransferases (Kleine *et al*, 2008; Otto *et al*, 2005). Polymer forming ARTDs contain an amino acid motif HYE in their catalytic core, whereas, proposed mono ARTDs have HYI/L/Y motif. ARTD9 and ARTD13 have QYT and YYV amino acid motifs respectively and likely their catalytic domains do not have ADP ribosylation activity (Kleine *et al*, 2008). Other ARTDs have not been studied in detail so far and more efforts are needed to characterize them.

1.1.1 ARTD activation, poly(ADP-ribosyl)ation reaction and ARTD catabolism

The most studied ARTD family member, ARTD1, is activated in response to the transient DNA strand breaks caused by various biological processes such as DNA replication, recombination, repair, damage and gene arrangement (Hassa & Hottiger, 2008). Other processes, which could activate the ARTDs are oxidative stress and DNA-binding drugs. Some of the activated ARTDs are capable of forming PAR polymers (Chambon *et al*, 1963). These PAR chains are negatively charged and their breakdown is mostly catalyzed by poly(ADP-ribose)

glycohydrolases (PARG) and ADP-ribosyl hydrolase-3 (ARH3) (Gagné *et al*, 2006; Oka *et al*, 2006). However, PARGs cannot remove the terminal ADP-ribose moiety present on the target proteins (Dunstan *et al*, 2012; Slade *et al*, 2011). The breakdown of ADP-ribose from the mono(ADP-ribosylated) proteins and also the catalysis of the last remaining ADP-ribose moiety are performed by ARH class of enzymes (Oka *et al*, 2006). Three proteins of the ARH family named ARH1-3 are expressed in mammals (Koch-Nolte *et al*, 2008). ARH1 function is to remove ADP-ribose moiety from ADP-ribosylated arginine residues whereas ARH3 hydrolyses the O-acetyl-ADP-ribose (Ono *et al*, 2006). It has been proposed that ARH3 is involved in the catalysis. Another protein that removes mono ADP-ribosylation from PARP modified proteins is terminal ADP-ribose protein glycohydrolase (TARG) (Sharifi *et al*, 2013).

1.2 ARTDs and their functions

1.2.1 ARTD1

The best studied and most characterized among ARTDs is ARTD1, which is a nuclear protein (Barth *et al*, 2006). However, a study where ARTD-related functions were disrupted by a ARTD antisense vector, suggested that ARTD1 could also be present in the mitochondria (Druzhyna *et al*, 2000; Scovassi, 2004). Human ARTD1 consists of six functionally distinct domains (**Fig. 2, Table 1**). The domain at the N-terminus is DNA binding domain (DBD) which is composed of two zinc fingers Zn1 and Zn2. They are involved in binding to DNA breaks by recognizing the DNA structures (D'Silva *et al*, 1999; Pion *et al*, 2003). The Zn3 domain is structurally different from Zn1 and Zn2 and is required for ARTD1 interdomain communication and also for condensing chromatin (Langelier *et al*, 2010, 2008); the automodification region (AR) forms the central part of the enzyme and comprises of breast cancer susceptibility protein C-terminus motif (BRCT), which is present in many DNA repair and cell cycle proteins (Bork *et al*, 1997) (**Fig. 2, Table 1**).

The AR also contains amino acid residues for the covalent attachment of PAR (Altmeyer *et al*, 2009b; Tao *et al*, 2009). ARTD1 contains WGR domain at the carboxy terminus of AR, which is rich in tryptophan, glycine and arginine. WGR is required for the DNA-dependent activity of ARTD1 (Altmeyer *et al*, 2009b). The C-terminal catalytic domain is further divided into two subdomains: the regulatory subdomain (RD) and the ADP-ribosyltransferase subdomain (ARTD). The ARTD domain catalyzes three different enzymatic reactions: initiation by attachment of the first ADP-ribose moiety to the acceptor protein, elongation of the chain by addition of ADP-ribose units and generation of the branching points. This catalytic domain marks the signature of the ARTD/PARP family and contains critical residues for NAD^+ binding and catalysis. The Zn1, Zn3, WGR and ARTD domains are essential for ARTD1 DNA-dependent activity (Altmeyer *et al*, 2009b; Langelier *et al*, 2012, 2011, 2008; Tao *et al*, 2008). Whereas,

deletion of Zn2 domain or BRCT motifs did not affect the DNA-dependent activity of human ARTD1 (Altmeyer *et al*, 2009a; Langelier *et al*, 2011).

ARTD1 acts as a DNA damage sensor and a signaling molecule binding to both single and double-stranded DNA breaks (Langelier *et al*, 2011). It has complex biological functions and is implicated in many cellular processes such as DNA repair (Malanga & Althaus, 2005), regulation of replication and differentiation (Yang *et al*, 2004), apoptosis and maintenance of genomic integrity (Koh *et al*, 2005), and in the expression of many proteins at transcriptional level (Hassa & Hottiger, 2008; Schreiber *et al*, 2006).
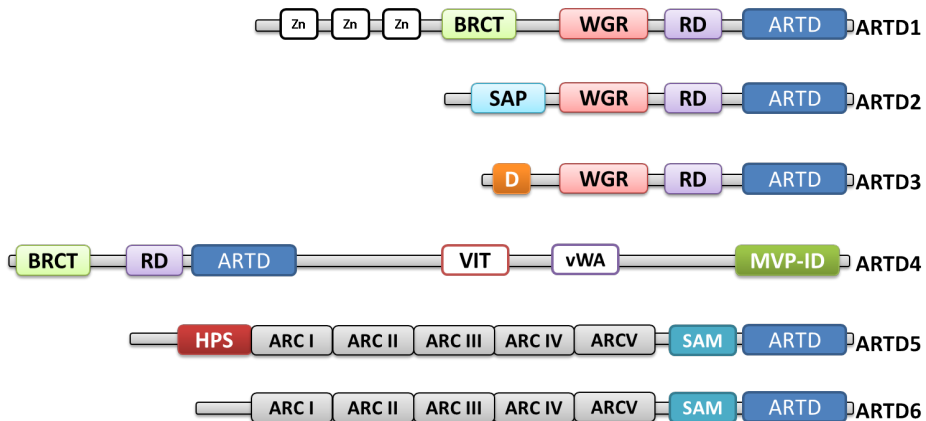
Figure 2. Domain organization of human ARTD superfamily members containing poly(ADP-ribos)ylation activity. The following domains are indicated; ARTD: catalytic ART domain, Zn: Zinc finger motif, BRCT: BRCA 1C Terminus domain, WGR: Tryptophan Glycine Arginine rich domain, RD: Regulatory domain, SAP: SAF/Acinus/PIAS-DNA-binding domain, D: DNA-binding motif, VIT: Vault protein inter-alpha-trypsin domain, vWA: von Willebrand type A, MVP-ID: Major-vault protein interaction domain, HPS: Histidine Proline Serine rich region, ARC: Ankyrin repeat clusters, SAM: Sterile-α motif.

1.2.2   ARTD2

ARTD2 is DNA-dependent nuclear protein (**Fig. 2, Table 1**). Out of all the ARTD members, ARTD2 is the closest relative to the founding member ARTD1 with 51 % identity in the catalytic ARTD domain. ARTD2 lacks the AR and its DNA binding domain (DBD) is different from ARTD1 (Amé *et al*, 1999; Oliver *et al*, 2004). Like ARTD1, it also contains the WGR and RD domain and has a catalytic domain at the carboxy terminus. The DNA binding domain of ARTD2 (SAP) shows no homology to any other ARTD reported and it may be responsible for the different substrate specificity in comparison to ARTD1 (**Fig. 2**) (Kutuzov *et al*, 2013; Oliver *et al*, 2004). The N-terminus also contains a

nuclear localization signal. The main role of ARTD2 is the same as of ARTD1 as it acts as a sensor and signaling molecule in response to DNA damage. ARTD2 has other proposed functions in genome integrity, spermatogenesis, adipogenesis and T cell development (Yélamos *et al*, 2008).

1.2.3 ARTD3

ARTD3 also contains a WGR domain as well as a catalytic domain (**Fig. 2, Table 1**). Some earlier studies have shown that unlike ARTD1 and ARTD2, ARTD3 is only moderately activated by DNA (Boehler *et al*, 2011). The main functions of ARTD3 are not well understood. However, it is thought to contribute to the cell division check point connecting the mitotic fidelity to the DNA damage (Augustin *et al*, 2003; Boehler *et al*, 2011).

Table 1. Human ARTD superfamily members and their characteristics. Molecular weights and amino acid length are indicated for canonical sequences.

ARTDs	Other names	Amino acids	MW (kDa)	ADP-ribosylation activity
ARTD1	PARP1	1014	113	Poly
ARTD2	PARP2	583	66	Poly
ARTD3	PARP3	533	60	Poly
ARTD4	PARP4	1724	193	Poly
ARTD5	PARP5a/TNKS1	1327	142	Poly
ARTD6	PARP5b/TNKS2	1166	123	Poly
ARTD7	PARP15	656	73	mono*
ARTD8	PARP14	1801	202	mono*
ARTD9	PARP9	854	96	inactive
ARTD10	PARP10	1025	110	mono
ARTD11	PARP11	331	39	mono*
ARTD12	PARP12	701	79	mono*
ARTD13	PARP13	902	101	inactive
ARTD14	PARP7	657	76	mono*
ARTD15	PARP16	322	36	mono*
ARTD16	PARP8	854	96	mono*
ARTD17	PARP6	630	71	mono*
ARTD18	TRPT1	253	28	mono*

*postulated activity

1.2.4 ARTD4

ARTD4 is located in the cytoplasmic vaults and is a component of the vault complex, a large cytoplasmic ribonucleoprotein (RNP) assembly (Kickhoefer *et al*, 1999). ARTD4 is larger in comparison to other known ARTD members (**Fig.**

2, Table 1). It comprises of five major domains, which are breast cancer susceptibility protein C terminus (BRCT) motif, catalytic ARTD domain, the vault protein inter-α-trypsin (VIT) domain, von Willebrand type A (vWA) and finally the major vault protein particle interacting domain (MVP-ID). BRCT domain is thought to bind phosphorylated DNA damage-sensing proteins (Manke *et al*, 2003). VIT and vWA domains are presumed to mediate protein-protein interactions, reviewed in (Hassa & Hottiger, 2008). It should be noted that ARTD domain is located close to the N-terminus in comparison to C-terminal in other ARTDs. MVP-ID as the name suggests interacts with the major vault protein. MVP mRNA levels are shown to be an indicator of the multi drug resistance (MDR), which is a major cause of chemotherapy failure in the cancer patients (Laurençot *et al*, 1997; Siva *et al*, 2001; Wittes & Goldin, 1986). ARTD4 is also present in the nucleus where it is not attached to the vault components (Kickhoefer *et al*, 1999). ARTD4 is loosely bound to the vault protein particle and it might have some other functions also. DNA damage does not activate ARTD4 and its biological roles are unknown so far.

1.2.5   Mono (ADP-ribosyl) transferases

As mentioned earlier, mono ADP-ribosyltransferases have amino acid substitutions in their catalytic centers and that enables them to attach just mono ADP-ribose moieties to the target proteins (Hottiger *et al*, 2010; Kleine *et al*, 2008). This subfamily comprises of ARTD7-ARTD17 excluding ARTD9 and ARTD13 which are described as inactive or pseudo ARTDs (**Table 1**). Mono(ADP-ribosyl) transferases do not contain the catalytic glutamate present in polymer forming ARTDs (HYE), which is required for elongation of the ADP-ribose chain (Otto *et al*, 2005). They are proposed to utilize the glutamate of the substrate protein and thus follow the substrate-assisted catalysis mechanism (Kleine *et al*, 2008). It has been indicated in several studies that mono ADP-ribosyltransferases play critical roles in intracellular signaling, transcription, immunity, inflammation, and stress response (Feijs *et al*, 2013).

1.3   Tankyrases

Tankyrases (TNKSs) are able to catalyze PARsylation reaction along with other PAR forming members (ARTD1-ARTD4). This subfamily contains two members, one is known as TNKS1 but also referred to as ARTD5 or PARP5a, likewise second member TNKS2 is also known as ARTD6 or PARP5b (**Fig. 2, Table 1**). Tankyrases are located in the cytoplasm and are more concentrated near the nuclear envelope and Golgi apparatus (Chi & Lodish, 2000; Smith *et al*, 1998). Tankyrases were first identified as the components of the human telomeric complex, known as shelterin complex (Smith *et al*, 1998). Tankyrases differ from other ARTD members because of their unique domain organization (**Fig. 2**).

TNKS1 and TNKS2 are very similar to each other in their domain construction. They contain a SAM domain (sterile alpha motif) which is required for the TNKS oligomerization and the characteristic catalytic ARTD domain that synthesizes the poly(ADP-ribose) units onto the acceptor proteins and to itself. The N-terminal consists of a region comprising of 24 ankyrin repeats, which are segmented into five ankyrin repeat clusters (ARC I-V). Ankyrin repeat clusters (ARCs) interact with the target proteins and their phylogenetic analysis showed that ARC III is less conserved in comparison to other ARCs (Seimiya *et al*, 2004). In another study, solution-based library screen was used and binding of tankyrase substrate c-Abl Src homology 3 domain-binding protein-2 (3BP2) with ARCs was studied. It was found that all the ARCs except ARC III were able to bind to 3BP2. Sequence alignment analysis of ARCs showed that ARC III lacks the conserved region that corresponds to the peptide-binding pockets (Guettler *et al*, 2011).

TNKS1 has an additional region at the N-terminal that contains the homo polymeric runs of histidine, proline and serine, thus named as HPS region. This additional region most likely has a regulatory function, although it is not well studied and its main function is unknown so far. The overall sequence identity between TNKS1 and TNKS2 is 82 % and sequence identity of the catalytic ARTD domain is 89 %. Unlike other polymerases, tankyrases do not contain an α-helical regulatory domain, which is required for the catalytic activity of ARTD1 in response to DNA damage.

1.3.1   Crystal Structure

The crystal structures of the catalytic domain of both the tankyrases have been solved, but complete structural information of the full-length tankyrases is not available so far. The catalytic ARTD domains of tankyrases have the same α/β fold as present in other ARTDs. They also contain a unique zinc binding region with an unknown function (**Fig. 3**) (Karlberg *et al*, 2010; Lehtiö *et al*, 2008). The tankyrase catalytic domain contains a characteristic ARTD signature motif (β-α-loop-β-α) (Bell & Eisenberg, 1997) as present in other ARTDs (**Fig. 3**). Tankyrases lack a 32-residue loop on the back side of ARTD domain, which is present in ARTD1 (Lehtiö *et al*, 2008). The catalytic ARTD domains of tankyrases have two different binding sites for NAD^+ and target protein. The analysis of crystal structures of ARTD1 and tankyrase ARTD domains have established that NAD^+ binding site is structurally equivalent among them. Furthermore, NAD^+ binding cavity can be subdivided into two distinctively different sites, one binding to the nicotinamide and other one binding to the adenosine moieties. This is where all of the reported inhibitors bind and most of the inhibitors actually occupy the nicotinamide-binding site (**Fig. 3**). The interactions shared by inhibitors binding at nicotinamide-binding site are discussed further in section 1.6.5.
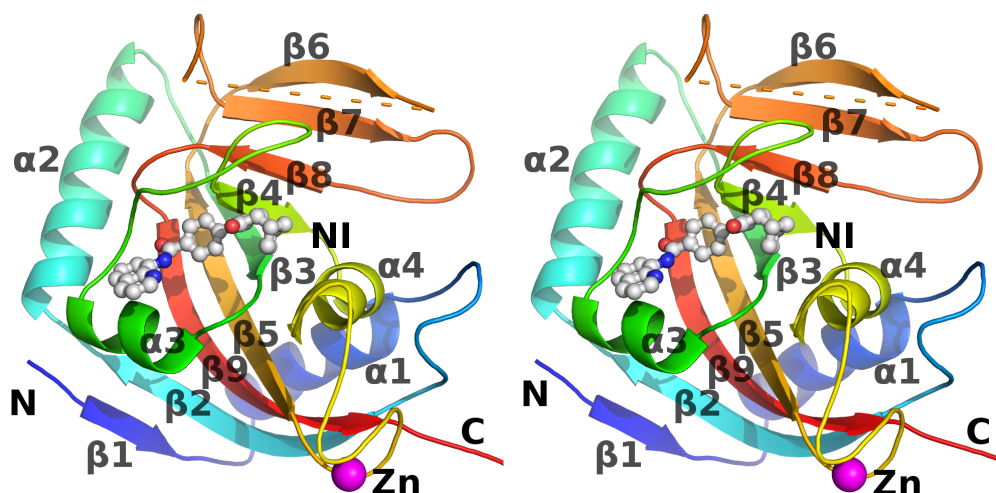
Figure 3. Stereo view of crystal structure of catalytic domain of human TNKS2 in complex with IWR-1. Tankyrase monomers are colored from blue at the N-terminus to red at the C-terminus. Nicotinamide binding site (NI), zinc atom (purple sphere) and secondary structural elements are labeled. The disordered loop is shown as a dashed line.

Notably, the NAD^+ bound crystal structure is not available yet for any of the ARTD-family members. As mentioned earlier, tankyrases are missing the regulatory domain that makes their NAD^+ binding site more exposed to the substrate in comparison to ARTD1-ARTD3. The NAD^+ binding site in the crystal structures of unbound catalytic domain is lined by a short sequence of amino acid residues that is commonly known as donor loop (D-loop) and it adopts different conformations in many ARTDs. The D-loops of tankyrases are identical in sequence but are present in different conformations in the solved crystal structures. In ligand free crystal structures of TNKS1 and TNKS2, D-loop is found in closed conformation. In case of TNKS1, the D-loop is closed near the nicotinamide site mainly by hydrophobic residues (Lehtiö *et al*, 2008), whereas in TNKS2, it is closed at the adenosine site by His1048 (Karlberg *et al*, 2010). However, analysis of co-crystal structures of tankyrases with bulky ligands showed that D-loop is flexible and opens up in order to accommodate the compounds (Haikarainen *et al*, 2013b; Narwal *et al*, 2013b, 2012b).

1.3.2   Tankyrase modifications

Tankyrases undergo post-translational modifications, which might be related to the regulation of their catalytic activities. TNKS1 is phosphorylated by various kinases such as mitogen-activated protein kinase (MAPK) (Chi & Lodish, 2000), glycogen synthase kinase 3 (GSK3) (Yeh *et al*, 2006b) and Polo-like kinase 1 (PLK1) (Ha *et al*, 2012). However, the exact molecular effects of these phosphorylations are not clear. MAPK modifies TNKS1 during insulin

stimulation but it does not appear to affect the glucose transporter type 4 (GLUT4)-mediated glucose uptake, where TNKS1 plays a role (Chi & Lodish, 2000). The phosphorylation by GSK3 seems to occur only during mitosis (Yeh *et al*, 2006b). PLK1 mediated phosphorylation appears to stabilize the TNKS1 levels and also increases its catalytic activity (Ha *et al*, 2012). Recently, it has been demonstrated that TNKS2 exhibits eight sites which are hydroxylated by the factor inhibiting hypoxia inducible factor (FIH)-catalyzed post-translational hydroxylation (Cockman *et al*, 2009). The exact functions of these post-translational modifications are also poorly understood. Auto-PARsylation of tankyrases provides a recognition signal that could be utilized for the ubiquitination by the WWE domain of the E3 ubiquitin ligase RING finger protein 146 (RNF146). Ubiquitination causes the proteasomal degradation of the PARsylated proteins (Callow *et al*, 2011; Zhang *et al*, 2011).

1.3.3   The SAM domain

The SAM domain has been demonstrated to be required for the optimal catalytic activity and also for the polymerization of tankyrases to assemble large protein complexes (De Rycker & Price, 2004). Auto-PARsylation causes the disassembly of oligomeric complexes of proteins. Tankyrases have been proposed as scaffolding molecules (Seimiya & Smith, 2002; Seimiya *et al*, 2004) and it is likely that they use SAM domains along with their respective catalytic ARTD domains to assemble and disassemble large protein frameworks at different locations in the cell (De Rycker & Price, 2004). It has also been shown previously that TNKS1 and TNKS2 associate with each other in *in vivo* (Sbodio *et al*, 2002). However, it is still need to be confirmed if this binding is established through SAM domains.

1.3.4   The ankyrin repeats and the target specificity

As mentioned earlier, tankyrases contain 24 ankyrin repeats which are further segmented into five ankyrin repeat clusters (ARC I - ARC V) (**Fig. 2**). These ankyrin repeat clusters (ARCs) are involved in the substrate binding *via* their multiple binding sites for the interacting partners. ARCs have potential redundancy in their functions as earlier studies have indicated that they, individually or in combination, were able to bind to tankyrase binding partners (Seimiya & Smith, 2002). ARCs have been shown to interact with a number of proteins and it has been established that a consensus binding motif (RXXPXG) is required for the binding; where arginine and glycine are at position 1 and 6 respectively, X denotes any amino acid, and there could be a small hydrophobic amino acid at position 4 (De Rycker *et al*, 2003; Guettler *et al*, 2011; Seimiya & Smith, 2002; Seimiya *et al*, 2004). Recently, a crystal structure of TNKS2 in complex with its Wnt signaling partner axis inhibition protein (Axin) was reported that showed that binding of other proteins could promote tankyrase dimerization (Morrone *et al*, 2012).

1.4   Functions of tankyrases

Tankyrases are present in a variety of human tissues and have been implicated in several functions. They are expressed in adipose tissue, kidney, thymus, brain, endocrine pancrease, skeletal muscle, spleen and are present abundantly in testis (Chiang *et al*, 2008; Yeh *et al*, 2009).

Table 2. List of some of the known tankyrase binding proteins

Protein	function(s)	Reference(s)
Telomere-repeat binding factor-1 (TRF1)	telomere binder factor and negative regulator of telomere length	(Smith *et al*, 1998)
AXIN1/2	tumor suppressor protein involved in Wnt signaling	(Huang *et al*, 2009)
Insulin-regulated aminopeptidase (IRAP)	insulin signaling pathway	(Chi & Lodish, 2000; Sbodio & Chi, 2002; Sbodio *et al*, 2002)
Glucose transporter (GLUT4)	glucose transporter	(Chi & Lodish, 2000),
Nuclear mitotic apparatus protein (NuMA)	spindle pole marker	(Chang *et al*, 2005a, 2005b; Sbodio & Chi, 2002)
182- kDa tankyrase binding protein (TAB182)	tankyrase binder with unknown function	(Sbodio & Chi, 2002)
Myeloid cell leukemia 1 (Mcl-1)	regulator apoptosis	(Bae *et al*, 2003)
Epstein- Barr nuclear region (EBNA1)	maintenance of the viral genome	(Deng *et al*, 2005, 2002)
Formin-binding protein 1 (FNBP1/FBP17)	nuclear phosphoproteins required for limb and renal development	(Fuchs *et al*, 2003)
Cancer susceptibility candidate 3 (CASC3)	regulate splicing , metabolism, export and localization of mRNA	(Zhang *et al*, 2011)
Basic leucine zipper nuclear factor 1 (BLZF1)	Maintenance of Golgi structure and protein transport	(Zhang *et al*, 2011)
c-Abl Src homology 3 domain-binding protein-2 (3BP2)	regulate signaling from immunoreceptors	(Levaot *et al*, 2011)

Table 3. List of some of the proposed tankyrase binding proteins

Protein	function(s)	Reference(s)
Growth factor receptor-bound protein 14 (GRB14)	regulate signaling	(Lyons *et al*, 2001)
A homeobox protein HOXB2	transcription factor	(Sbodio & Chi, 2002)
Polymorphic variant of the protein phosphatase 1 regulated subunit 12 C (PP12C)	regulates myosin phosphatase activity	(Sbodio & Chi, 2002)
Tax1-binding protein 1 (TAX1BP1)	apoptosis regulation	(Sbodio & Chi, 2002)
Alpha 1S subunit of the voltage-dependent L-type calcium channel (CACNA 1S)	regulate excitation-contraction coupling in skeletal muscles	(Sbodio & Chi, 2002).
Ubiquitin-specific protease 25 (USP25)	involved in cell cycle regulation and stress response	(Sbodio & Chi, 2002).

A diverse range of tankyrase binding proteins are reported and with some of them the interactions are well characterized (**Table 2**). In addition, several proteins have been proposed to contain a tankyrase binding motif RXXPXG (De Rycker *et al*, 2003; Guettler *et al*, 2011; Seimiya & Smith, 2002; Seimiya *et al*, 2004). A few of them are listed in **Table 3**. This indicates that tankyrases have many roles in the cell and some of the best-characterized functions of the tankyrases will be discussed in detail in the following paragraphs.

1.4.1   Telomere maintenance

Telomeres are protective noncoding repetitive nucleotide sequences at the ends of the eukaryotic chromatids. They cannot be replicated by the DNA replication machinery because of the end replication problem (Counter *et al*, 1994). As a consequence of this, telomeres become shorter after each replication cycle unless synthesized by a telomerase enzyme. Telomerase is a reverse transcriptase containing its own RNA template and a catalytic subunit. In most of the human cells, the activity of the telomerase is repressed.

However, it is found to be upregulated in some normal cells and in almost all types of cancers (Shay & Bacchetti, 1997). Telomeres consist of TTAGGG repeats and are protected by shelterin complex. Shelterin complex is composed of telomere repeat factor 1 (TRF1), telomere repeat factor 2 (TRF2), protection of telomeres 1 (POT-1), TRF interacting protein 2 (TIN2), tripeptidyl-peptidase 1 (TPP1), and repressor/activator site-binding protein (rap1) (**Fig. 4**). In the absence of shelterin complex, telomeres would be inappropriately processed by DNA damage surveillance machinery. TNKS1 plays a central role at the telomeres by binding to TRF1 (Smith *et al*, 1998).
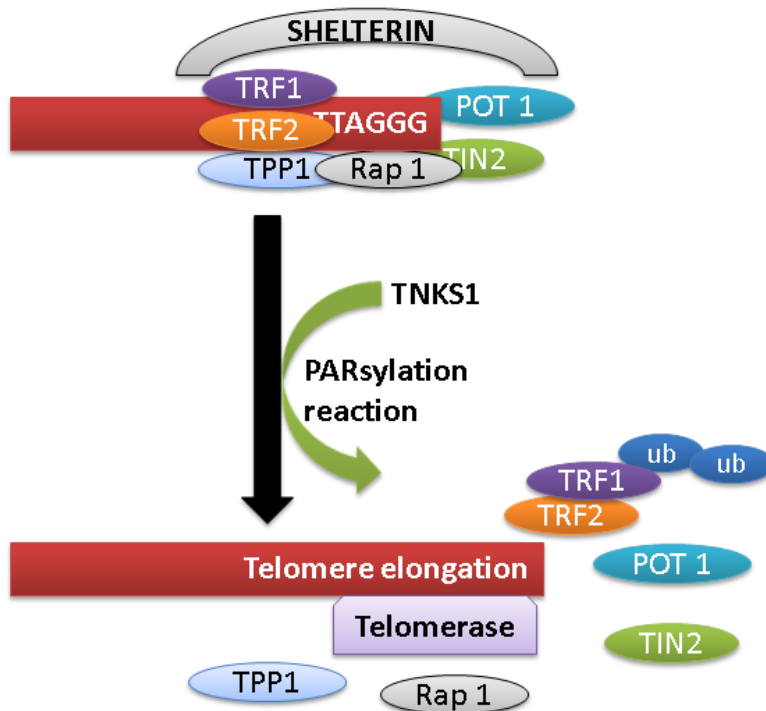
Figure 4. Telomere elongation by TNKS1. Telomeres are protected by Shelterin complex consisting of TRF1, TRF2, TPP1, Rap1, Pot1 and TIN2. TNKS1 PARsylates TRF1 and removes it from the telomeres, this gives access of telomeres to telomerases. Modified TRF1 is further ubiquitinated before undergoing to proteosomal degradation.

TRF1, which is part of shelterin complex, blocks the access of telomeres to telomerases and therefore serves as a negative regulator of the telomere length (Palm & de Lange, 2008). Ankyrin repeats of tankyrases contain a TRF1 binding site in ARC V subdomain (Seimiya *et al*, 2004). The catalytic ARTD domain PARsylates TRF1 (Smith *et al*, 1998) and adds negative charge to TRF1, reducing its ability to bind telomeres. Consequently, the telomeres become

accessible to telomerases, while released TRF1 is ubiquitinated and subjected to proteasomal degradation (**Fig. 4**) (Her & Chung, 2009; Lee *et al*, 2006). Consistent with these observations, it has also been shown that telomere elongation and shortening could be induced by the overexpression and suppression of TNKS1, respectively (Cook *et al*, 2002; Donigian & de Lange, 2007; Seimiya *et al*, 2005; Smith & de Lange, 2000). Long telomeres are typical in cancer cells and inhibition of telomerase has been proposed as a potential therapeutic strategy (Seimiya *et al*, 2005). Moreover, inhibition of the human tankyrases by non-specific inhibitors such as 3-aminobenzamide (3-AB) and PJ-34 enhance telomere shortening (Seimiya, 2006). Therefore, a combinatorial approach to inhibit telomerases and tankyrase might be beneficial in the cancer therapy.

1.4.2 Role in Wnt signaling pathway

Wnt signaling pathway plays essential roles in embryonic development, cell fate specification, stem cell regeneration, neuronal migration and in the adult tissue homeostasis (MacDonald *et al*, 2009). Wnt proteins are signaling molecules that are involved in the cell-to-cell interactions during embryogenesis.
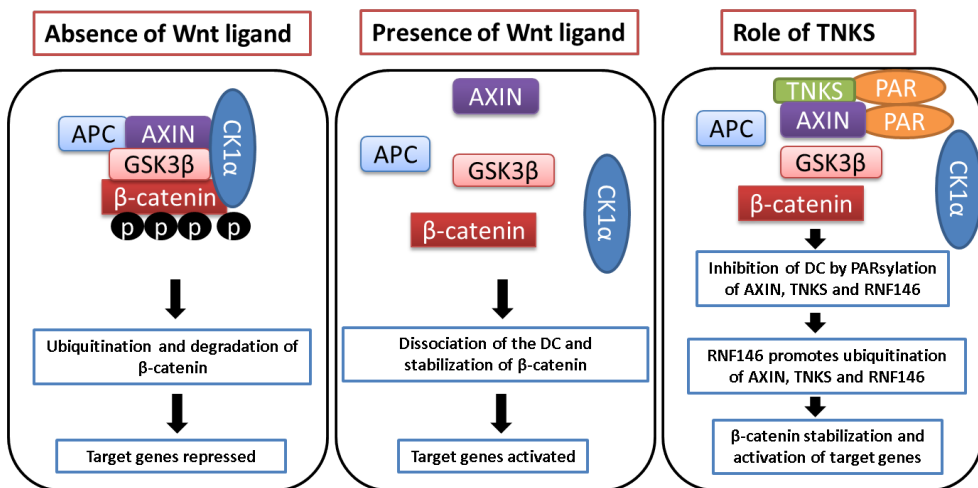
Figure 5. Role of TNKSs in Wnt signaling. In the absence of Wnt ligand, β –catenin destruction complex (BCDC) remains intact and causes the degradation of β-catenin. Whereas in the presence of a Wnt ligand, BCDC members dissociate and leads to the stabilization of β-catenin and finally activation of the target genes. TNKSs modifies AXIN and causes the stabilization of β-catenin.

Inappropriate activation of Wnt signaling pathway has been implicated in many cancers (Polakis, 2007, 2000). A striking feature of the Wnt pathway is its

involvement in the regulated proteolysis of the transcriptional co-activator β-catenin. In the absence of Wnt signaling, a protein complex, known as β-catenin destruction complex, regulates signaling and β-catenin levels. This complex is composed of adenomatous polyposis coli (APC), glycogen synthase kinase (GSK3β), cyclin-dependent kinase (CK1α, CK1δ and CK1ε) and axis inhibition protein (Axin1/2). Axin has been proposed as the concentration limiting component in the regulation of the β-catenin degradation (Huang *et al*, 2009).

GSK3β phosphorylates β-catenin and causes its proteasomal degradation (Hart *et al*, 1999). The Wnt signaling pathway recruits the GSK3β and Axin to the plasma membrane. Due to this the β-catenin destruction complex dissociates and non-phosphorylated β-catenin levels increase in the cells (**Fig. 5**). Truncation mutations in either tumor suppressor gene *APC* or *CTNNB1* (the gene encoding β-catenin) have been implicated in 95 % of the colorectal cancers. Tankyrases play a central role in the regulated degradation of the β-catenin by modifying Axin. They regulate the levels of Axin, RNF146 and themselves *via* PARsylation reaction (Callow *et al*, 2011; Huang *et al*, 2009; Waaler *et al*, 2012). RNF146 is a ring-domain E3 ubiquitin ligase that acts as a positive regulator of Wnt signaling. It controls the degradation of Axin, tankyrases and itself by recognizing the tankyrase-mediated PARsylation (**Fig. 5**) (Callow *et al*, 2011; Zhang *et al*, 2011). Hence, tankyrases are the key molecules in maintaining the cellular levels and turnover number of β-catenin. It has been reported that inhibition of the catalytic activity of tankyrases cause the inhibition of the Wnt signaling and consequently the stabilization of the Axin (Huang *et al*, 2009). Notably, tankyrase-Axin interactions are also involved in insulin-stimulated glucose uptake.

1.4.3 GLUT4 vesicle translocation

GLUT4 is one type of a glucose transporter, which is mostly expressed in the skeletal muscles and adipose tissues (Hou & Pessin, 2007; Leney & Tavaré, 2009). In the basal state, GLUT4 resides in the intracellular membrane components known as GLUT4 storage vesicles (GSVs). Interestingly, GSVs also contain a tankyrase binding protein IRAP (Chi & Lodish, 2000). GLUT4 and IRAP play a central role in the insulin-stimulated glucose uptake (Guo *et al*, 2012). When blood glucose levels rise, insulin secretion is elevated subsequently stimulating the glucose uptake by inducing rapid translocation of GLUT4 vesicles to the cell membrane. It has been demonstrated that TNKS1 binds to IRAP and facilitates the exocytosis of GSVs. Knocking down of either TNKS1 or IRAP suppresses the GLUT4 translocation (Yeh *et al*, 2007).

Immunoprecipitation experiments and *in vitro* pull down assays indicated that TNKS2 forms a ternary complex with Axin and kinesin motor protein (KIF3A) (Guo *et al*, 2012). To confirm that TNKS2-AXIN-KIF3A complex is required for GLUT4 translocation in response to insulin, immunofluorescent staining was carried out in differentiated adipocytes cells expressing high levels of GLUT4.

Results showed that in the absence of insulin, the ternary complex co-localizes with GLUT4 in the adipocytes. However, in the presence of insulin, the distribution of GLUT4 was observed at the cell surface (Guo *et al*, 2012). Knocking down the each component of the ternary complex indicated that all the components are essential for the active transport of GLUT4, and absence of any of them could suppress the translocation of GLUT4 and glucose uptake following insulin stimulation (Guo *et al*, 2012).

In the absence of insulin, tankyrase proteins PARsylate themselves, axin and GLUT4, causing their subsequent ubiquitination. Insulin signaling inhibits tankyrase activity and this further stabilizes the ternary complex (Guo *et al*, 2012). The potent tankyrase inhibitor XAV939 seems to have similar effect as insulin, which indicated that tankyrase PARsylation activity plays a negative role in mediating the stability of translocation complex. Although the role of tankyrases in this particular process is elusive and needs further research (Guo *et al*, 2012).

1.4.4 Mitosis

In the earlier studies, tankyrases have been shown to PARsylate several proteins that are involved in mitosis (Chang *et al*, 2005a, 2005b; Kim *et al*, 2012). This suggests that tankyrases have a functional role in the cell cycle. TNKS1 localizes at the spindle poles during mitosis and its activity is also upregulated during the process. Knocking down TNKS1 by RNA interference causes pre-anaphase arrest (Dynek & Smith, 2004). Notably, some of the proteins involved in mitosis and modified by tankyrases are NuMA (Chang *et al*, 2005a, 2005b; Dynek & Smith, 2004) and Miki (Ozaki *et al*, 2012). NuMA is a nuclear protein, which is associated with mitotic apparatus and shuttles between the nuclear matrix in interphase and the spindle poles in mitosis. NuMA plays a central role in many processes such as in the nuclear structure, spindle assembly, and nuclear re-formation (Chang *et al*, 2005b). PARsylation of NuMA by tankyrases has been proposed to be essential for maintaining proper spindle polarity (Chang *et al*, 2005a; Hsiao & Smith, 2008). Miki is a mitotic kinetics regulator that resides in the Golgi apparatus and translocate to the mitotic centrosome in late G2 and prophase (Ozaki *et al*, 2012). Depletion of Miki induces prometaphase arrest that consequently leads to chromosome scattering and pseudo metaphase. TNKS1 is activated by phosphorylation through GSK3β (Yeh *et al*, 2006a) and it PARsylates Miki (Ozaki *et al*, 2012). This modification is required for the translocation of Miki from Golgi apparatus. Tankyrases and PARsylated Miki translocate together in the late G2 to prophase where Miki anchors the scaffold protein CG-NAP (centrosome and Golgi localized protein kinase N-associated protein).

TNKS1, Miki and CG-NAP are required for the formation of robust microtubules and subsequently for the normal movement of chromosomes in the

prometaphase. Their downregulation leads to prometaphase defect (Ozaki *et al*, 2012). During interphase, TNKS1 forms a complex with GDP-mannose 4,6–dehydratase (GMD). Unlike other binding partners, GMD does not get modified, but it inhibits TNKS1 activity and this complex may serve as the ready pool of inactive TNKS1 (Bisht *et al*, 2012). It has also been proposed that TNKS1 binding to NuMA or TRF1 is inhibited by GMD and phosphorylation of TNKS1 *via* GSK3β might have a role in breaking the TNKS1-GMD complex (Bisht *et al*, 2012). Along with GSK3β, another kinase protein Polo-like-kinase (PLK1) is also identified as tankyrase binding partner at the telomeres. PLK1 is a serine/threonine kinase that increases the TNKS1 stability and its PARsylating activity at the telomeres by phosphorylation reaction (Ha *et al*, 2012). ARTD3 also plays a critical role in the stabilization of the mitotic spindle and in promoting the telomere integrity. It is found to be a positive regulator of TNKS1 mediated modification of NuMA in a DNA independent manner and also enhance the automodification of TNKS1 (Boehler *et al*, 2011).

Another aspect of tankyrases that make them important players in the mitosis is their function at the centrosome. Tankyrases have been implicated in the regulation of centrosome duplication process which is critical for the genome integrity. A centrosomal P4.1-associated protein (CPAP) is required for the normal centrosome function in the human cells. Earlier, it was reported that down regulation of CPAP prevented centrosome duplication and its overexpression led to aberrant centriole elongation, supernumerary centrioles and spindle multipolarity (Kim *et al*, 2012). Thus, regulation of CPAP levels is very critical for the normal cell cycle. Notably, CPAP is a binding partner of tankyrases and its stability and function at the centrosomes is regulated by the tankyrase-mediated PARsylation reaction.

Altogether, the involvement of the tankyrases in the aforementioned processes makes them key players in the mitosis and cell cycle.

1.4.5   Proteasome regulation

ADP-ribosylation by tankyrases is identified as a regulator of protein degradation by the ubiquitin-proteasome system (UPS) (Cho-Park & Steller, 2013). Protein degradation is the primary means for the removal of misfolded and potentially toxic proteins. Abnormal protein degradation is associated with several human diseases such as muscle-wasting diseases, neurodegenerative disorders and cancer (Glickman & Ciechanover, 2002; Goldberg, 2007; Hershko & Ciechanover, 1998). The UPS mainly carries out selective protein degradation. In this process, proteins are tagged with the polyubiquitin chains and these tagged proteins are further hydrolyzed into small peptides by the 26S proteasome. The 26S proteasome is a large protease complex, composed of 20S core particle and 19S regulatory particles, and its activity is regulated by large number of loosely associated proteins. One such regulator is proteasome inhibitor 31 (PI31) that

was identified as an inhibitor of 20S core particle and as an activator of 26S proteasome activity (Bader *et al*, 2011; Chu-Ping *et al*, 1992; McCutchen-Maloney *et al*, 2000).

Tankyrases modulate PI31 activity *via* PARsylation and this modification further reduces the affinity of this protein for binding to the 20S particle (Cho-Park & Steller, 2013). Moreover, chaperons, dp27 and dS5b, associated with 19S particles are also found as the binding partners of PI31. In this particular process, tankyrase-mediated PARsylation causes increased binding of PI31 to dp27 and dS5b and subsequently promotes the 26S proteasome assembly. Inhibition of tankyrases reduce the 26S proteasome activity in both Drosophila and mammalian cells (Cho-Park & Steller, 2013). Therefore, tankyrase activity plays an important role in the regulation of protein degradation *via* UPS and abnormal degradation could be targeted by tankyrase inhibition.

1.5   Role of tankyrases in cancer

Increased expression of the tankyrases has been detected in many cancers such as fibrosarcoma (Smith *et al*, 1998), ovarian cancer (McCabe *et al*, 2009), glioblastoma (Shervington *et al*, 2007), pancreatic adenocarcinoma (Zhao *et al*, 2009), breast cancer (Gelmini *et al*, 2004; McCabe *et al*, 2009; Smith *et al*, 1998), lung cancer (Busch *et al*, 2013), astrocytoma (Tang *et al*, 2012), transitional cell carcinoma of the bladder (Gelmini *et al*, 2004), gastric cancer (Gao *et al*, 2011) and colon cancer (Gelmini *et al*, 2006). However, a study on the colon cancer showed that TNKS1 was up-regulated and TNKS2 was down-regulated in comparison to the normal cells (Shebzukhov *et al*, 2008). Furthermore, mutations such as deletion or duplication of nucleotides in the DNA coding sequence of the tankyrases are also seen in gastric and colorectal cancers (Kim *et al*, 2011). A recent study has also established tankyrases as potential drug targets in the colorectal carcinomas (CRCs) *in vitro* and *in vivo* (Lau *et al*, 2013). Two inhibitors, G007-LK and G244-LM, were used to specifically inhibit tankyrases in order to attenuate Wnt signaling and consequently promote the β-catenin degradation. G007-LK binds to the adenosine site of the tankyrases, whereas G244-LM binds to the nicotinamide site.

These tankyrase inhibitors completely blocked the ligand driven Wnt signaling in the normal cells and displayed approximately 50 % inhibition in the APC mutation-driven signaling (Lau *et al*, 2013). Out of the two compounds, G007-LK was more selective and was also able to inhibit *in vivo* tumor growth in an APC-mutant CRC model. In some of the *KRAS*-mutant cell lines, G007-LK did not show single-agent activity for the inhibition of the clonogenic cell growth. However, it potentiated the effect of mitogen activated kinase (MEK) inhibitor (Lau *et al*, 2013). Recently, tankyrases were also implicated in lung cancers (Casás-Selves *et al*, 2012). The most common type of lung cancer is adenocarcinoma, which is the result of the mutations in the epidermal growth factor receptor (EGFR) gene. Although, EGFR inhibitors are sufficient for the

treatment, there are some cases, where cancer cells developed a particular escape mechanism to promote the cell survival. One such mechanism is *via* Wnt signaling pathway which is positively regulated by tankyrase-mediated modifications. Inhibition of tankyrases, in these cases, has increased the activity of EGFR inhibitors both *in vivo* and *in vitro* (Casás-Selves *et al*, 2012). In addition, tankyrases are also involved in the breast cancers associated with the decreased expression of either breast cancer type 1 susceptibility protein 1 (BRCA1) or BRCA2. Tankyrase inhibition in these cells was synthetic lethal and was characterized by the increase in the centrosome amplification, whereas there was no effect in the control cells. The basis of the mechanism causing this synthetic lethality is so far not understood. (McCabe *et al*, 2009).

1.5.1 Role of tankyrases in viral infections

Tankyrases are also implicated in viral infections such as in the replication of herpes simplex virus (HSV) (Li *et al*, 2012). Tankyrase acts as a target of HSV and undergoes phosphorylation, nuclear translocation and degradation. Post-HSV infection, TNKS1 was phosphorylated by MAPK and was also recruited to the nucleus of HSV infected cells. TNKS1 co-localized with the HSV-infected cell polypeptide (ICP0) in the nucleus and their interaction is required for the HSV replication. In the normal cells, ICP0 regulates nuclear localization of TNKS1, whereas in case of infection, viral protein expression leads to the recruitment of TNKS1 into the nucleus. The replication of herpes simplex virus type 1 (HSV-1) was impaired when both TNKS1/2 were knocked out using siRNA. Similar effects were seen when tankyrase enzymatic activity was inhibited using XAV939 treatment. These results indicated that HSV-1 replication was promoted by the catalytic activity of tankyrases (Li *et al*, 2012). In contrast, tankyrase has been shown to inhibit the replication of the Epstein-Barr virus origin of plasmid (Deng *et al*, 2005).

1.5.2 Role of tankyrases in obesity and other diseases

Tankyrases have also been proposed to be associated with obesity. Previously, 16 genetic loci have been linked to obesity using genome-wide association studies (Hinney & Hebebrand, 2009; Hofker & Wijmenga, 2009; Walley *et al*, 2009). In addition to this, during a meta-analysis study, two new genetic loci were identified that were relevant for early onset extreme obesity. One of them is present at a genetic locus between the tankyrase and methionine sulfoxide reductase, a gene that might be responsible for the obesity (Scherag *et al*, 2010).

Tankyrase knockout mice exhibit an increase in energy utilization and insulin-stimulated glucose utilization (Yeh *et al*, 2009). Tankyrases are also implicated in fibrotic disease as their inactivation by XAV939 or SiRNA effectively abolished the Wnt signaling and demonstrated antifibrotic effects (Distler *et al*, 2012). Cherubism, an autosomal-dominant syndrome, is also shown to be related

with the tankyrases. This disease is caused by the mutation in a gene that encodes 3BP2 (an adaptor protein), and 3BP2 stabilization is regulated by the tankyrase-mediated PARsylation reaction. Mutated 3BP2 escapes the tankyrase-mediated modification that further causes the stabilization of 3BP2 and subsequently signaling pathways get inappropriately activated. Therefore, cherubism is the result of the loss of interaction between the tankyrases and 3BP2 (Guettler *et al*, 2011; Levaot *et al*, 2011).

1.6 Drug development and available ARTD inhibitors

In this thesis, early drug-discovery efforts are made in order to identify potent and selective tankyrase inhibitors. Following sections will describe the general properties required for a drug candidate, clinical phases which a drug candidate has to pass, and finally summary of the discovery process that has led to currently available ARTD inhibitors.

1.6.1 Properties of a drug candidate and screening strategy

Drug designing is the process of finding out new small molecules that would be able to change the biological activity of the drug target and would also have therapeutic potential. Drug targets could be enzymes, receptors, ion channels, transporters or DNA. Before a drug is designed, there should be a method to screen the compounds against drug target. After establishing the testing procedures and finding the lead compound, structure-activity relationship studies are done and a pharmacophore is identified. Further, targeting interactions are modified using drug designing approaches that include laboratory experiments and computer aided methods.

In the laboratory experiments, chemical libraries containing large number of compounds are screened against the target molecule using biochemical assay. Computer aided methods could be further divided into three subclasses; inspection-based, virtual screening, and de novo generation. In inspection-based method, known molecules that bind the site are modified to become inhibitors. Virtual screening involves the screening of small-molecule libraries, in order to identify those structures, which are most likely to bind to the drug target. *De novo* generation method involves screening of small fragments of compounds and scoring them according to their interactions in the binding cavity. Later a complete compound is synthesized in the laboratory using screened small fragments.

However, it may take many years of research and development before a drug reaches the market.

1.6.2   Pharmacodynamics and pharmacokinetics

The pharmacological activity of a compound is defined by four benchmarks which are absorption, distribution, metabolism and excretion. These are generally abbreviated as ADME in pharmacology. A rule that describes these properties of a drug lead and also determine the druglikeness of the compound is known as Lipinski's rule of five (LRO5). This rule is followed during the drug discovery and helps in the stepwise optimization of the hit compounds. LRO5 facilitates the research process and increase the probability of converting a drug lead into an orally active drug. Rule of five is as follows:

  I.   There should not be more than 5 hydrogen bond donors.
  II.   There should not be more than 10 hydrogen bond acceptors.
  III.   Molecular mass should be less than 500 daltons.
  IV.   *logP* value should not be greater than 5.

1.6.3   Clinical phases

Drug candidates pass through different clinical phases before they reach the market. These phases include preclinical studies, phase 0, and phase I to phase V. In the preclinical studies, *in vitro* and *in vivo* experiments are performed in order to collect the information about the potency, efficacy, pharmacokinetics and safety of the compound. In phase 0 trials, small doses of drug is given to small population (10-15) of humans. The aim of phase 0 trial is to gather preliminary data about whether drug reaches the diseased cells, how drug behaves in the body and how diseased cells respond to the drug. This phase helps in speeding up the drug-development process. Phase I trails are generally performed on healthy individuals (20-100) in tightly controlled clinics. This phase is designed to collect data about the safe dose range, side effects, pharmacokinetics and pharmacodynamics of a drug.

Drugs that pass phase I trial, enter in phase II, where biological activity of the drug is tested. These tests are performed on a larger group (100-300) of patients and volunteers, and information about efficacy and toxicity is collected. In phase III trials, effectiveness of the drug is compared with the already existing standard treatment. This phase is also known as pre-marketing phase and drugs are required to be effective at this stage in order to obtain approval from the appropriate regulatory agencies. Phase IV trials involve the pharmacovigilance after drug has been shown to work and has been granted a license. Aim is to find out the long term risks and benefits over the larger patient population and longer time periods. Phase V is designed to determine if the significance of the new drug candidate is realized in clinical practice.

1.6.4 PARP inhibitors and selective tankyrase inhibitors

The PARP/ARTD family proteins are involved in several cellular processes and critical functions of some of the members has made them potential therapeutic targets. Nicotinamide, which is released during the PARsylation reaction was the first identified ARTD inhibitor (Clark *et al*, 1971). In 1980, more ARTD inhibitors (substituted benzamides) were identified (Purnell & Whish, 1980) and since then several novel scaffolds have appeared in context of various areas such as cancer therapy, cardiac ischemia, rheumatoid arthritis, stress response and diabetes mellitus (Gonzalez-Rey *et al*, 2007; Hilton *et al*, 2013; Pacher *et al*, 2002; Pyriochou *et al*, 2008; Szabó *et al*, 1997; Zingarelli *et al*, 1998). Most of the inhibitors discovered to date mimic nicotinamide and bind to the nicotinamide-binding site.

However, it was recently reported that some of the inhibitors were binding to adenosine site of tankyrases (IWR-1 and JW55). The most studied family member, ARTD1, has also been the most actively targeted ARTD member in the drug discovery research. However, because of the conserved nicotinamide-binding site, it is very likely that these inhibitors would inhibit other ARTD members also. As this research was on going, other ARTDs, such as tankyrases, were also getting attention because of the growing understanding of their biological roles. Notably, there were no selective tankyrase inhibitors available when this PhD project was started. During the project several groups including ours published many tankyrase inhibitors (Bregman *et al*, 2013a, 2013b; Huang *et al*, 2006; James *et al*, 2012; Shultz *et al*, 2013a, 2013b, 2012; Waaler *et al*, 2011; Yashiroda *et al*, 2010, 2010). Like ARTD1, the vast majority of the identified tankyrase inhibitors bind to the nicotinamide site but it was the different conformations of D-loop that provided the route for the development of selective tankyrase inhibitors by allowing binding of compounds to the adenosine site.

Inhibitor studies were further facilitated by the availability of the crystal structures of the catalytic domains (PDB codes: TNKS1, 2RF5; TNKS2, 3KR7) (Karlberg *et al*, 2010; Lehtiö *et al*, 2008). Compounds XAV939 and IWR-1 were found to inhibit Wnt signaling through tankyrase inhibition (Huang *et al*, 2009). Later crystal structures of TNKS2 in complex with XAV939 and IWR-1 were solved that helped in the understanding of their structure-activity relationships (Karlberg *et al*, 2010; Narwal *et al*, 2012b).

1.6.5 Tankyrase inhibitors binding to the nicotinamide site

The nicotinamide site is targeted by most of the tankyrase inhibitors such as XAV939 (**Fig. 6**) and they share some common features. Tankyrase and ARTD inhibitors form typical hydrogen bonds with Gly1032 and Ser1068 which are present at the bottom of the pocket in TNKS2 (Gly1185 and Ser1121 in TNKS1).

Another shared interaction is π-π stacking with Tyr1071 of TNKS2 (Tyr1224 in TNKS1). There has been efforts to optimize inhibitors binding to nicotinamide site (Haikarainen *et al*, 2013b; Shultz *et al*, 2013a, 2012).

1.6.6 Adenosine site and dual-site binding inhibitors

Some of the inhibitors do not contain nicotinamide motif, one such compound is IWR-1 (**Fig. 6**), which was discovered in Super top flash (STF) luciferase assay. STF assay is a cell-based assay that utilizes a construct containing luciferase TCF (T Cell Factor) reporter plasmid that responds to the Wnt/β-catenin pathway activity. IWR-1 was found as an antagonizer of Wnt signaling and later established as a selective tankyrase inhibitor (Huang *et al*, 2009). Complex crystal structure of TNKS2 with IWR-1 showed that it binds to the adenosine site (Narwal *et al*, 2012b).
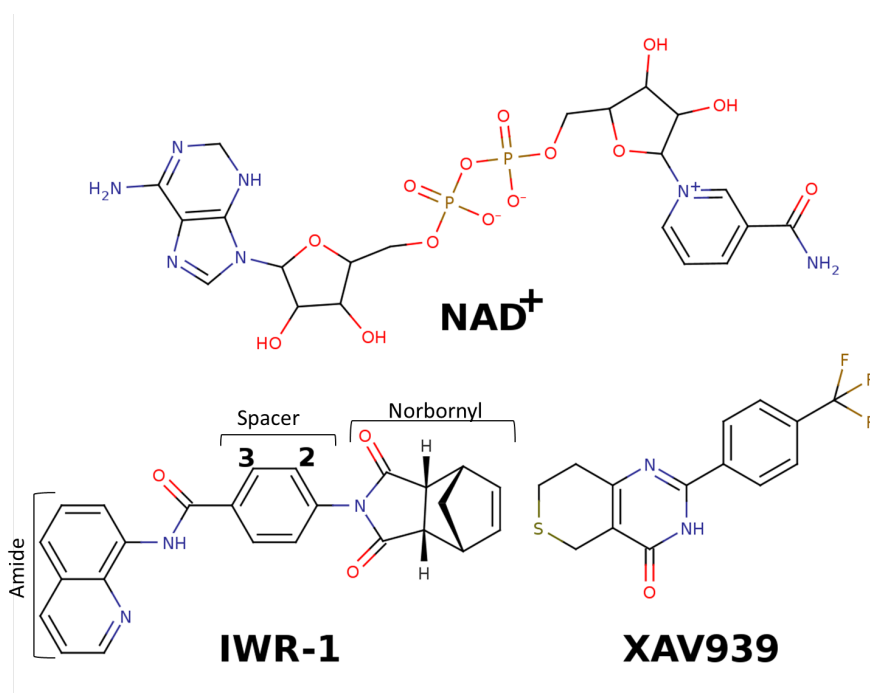
Figure 6. Chemical structure of NAD$^+$ along with the known potent TNKS inhibitors IWR-1 and XAV939. IWR-1 binds to adenosine site of the protein molecule and XAV939 binds to nicotinamide site. Different regions present in IWR-1 are mentioned.

The molecular basis of its interaction will be discussed later in the results and discussion chapters. Additionally, some more inhibitors were reported to bind to the adenosine site such as WIKI4, JW55, JW74, G007-LK (Bregman *et al*, 2013a, 2013b; Haikarainen *et al*, 2013b; Voronkov *et al*, 2013). One of the

ARTD inhibitors, PJ34, has been shown to bind to both the adenosine and the nicotinamide sites with one molecule binding to each site (Kirby *et al*, 2012). Recently, a novel class of tankyrase inhibitors were discovered that bind to both the nicotinamide and adenosine sites (Shultz *et al*, 2013a). These findings have led to the development of several chemical scaffolds as selective and potent tankyrase inhibitors.

2 Aims of the study

The primary aim of this thesis work was to develop selective and potent tankyrase inhibitors. Recognition of key roles that tankyrase play in multiple pathological conditions, including cancer, has led to efforts to develop effective inhibitors against them, as there were no specific tankyrase inhibitors available when this study was started. In order to identify potential hit compounds, chemical libraries were screened and potencies were measured using biochemical assay. Complex crystal structures with ligands were determined using macromolecular X-ray crystallography.

More specifically, in paper **I**, the aim was to develop an assay for human tankyrases that could be utilized for the screening of chemical libraries. Another plan was to validate the assay conditions and to carry out a validatory screening to verify that assay is working. Based on these results, in paper **III**, the goal was to screen a larger flavonoid library and discover novel inhibitors of tankyrases among different classes of flavonoids. In paper **IV**, the aim was to screen a small library of flavones with single substitution because flavones were the only class of flavonoids that was inhibiting tankyrase effectively. To evaluate the efficacy and selectivity of the hit compounds, we aimed to test compounds in cell based assay and against a panel of ARTD-family members available in our laboratory. In paper **III** and **IV**, we were aiming to measure the potencies of hit compounds and solve the co-crystal structure of the ligands with tankyrase 2 catalytic domain to establish the structure-activity relationship.

In Paper **II**, the aim was to solve a complex crystal structure with a potent tankyrase inhibitor, IWR-1, as this compound does not contain nicotinamide-binding motif. Another goal was to shed light on the molecular interactions between the substrate NAD^+ and tankyrases. There was no structural information available about the binding of substrate with any of the ARTD superfamily members, and substrate complex could give important information about the enzyme function. In paper **V**, aim was to evaluate the inhibition of tankyrases by known ARTD inhibitors using activity assay and protein X-ray crystallography.

3 Materials and methods

The materials and methods that were used in studies are described in full details in the respective publications (**I-V**). Only a short description is given here on the experimental approaches used.

3.1 Expression vectors (I-V)

The expression constructs of the catalytic fragment of human TNKS1 consisting of SAM and ARTD domain (1030-1317) and TNKS2 ARTD domain (946-1161) were gifts from Structural Genomics Consortium (SGC), Stockholm, Sweden. The coding sequences were cloned to a pNIC28-Bsa4 plasmid, which contains an N-terminal 6x-histag followed by a TEV protease cleavage site before the tankyrase sequence. TNKS2 fragment containing the SAM and ARTD domain and ARTD1, ARTD2, ARTD4, ARTD7, ARTD10, ARTD12 were either obtained from SGC or produced in our laboratory by the members of the research group (Haikarainen *et al*, 2013b; Narwal *et al*, 2013b).

3.2 Protein expression and purification (I-V)

Protein expression for all the tankyrase constructs was conducted in the *E. coli* (Rosetta 2 DE3) cells using terrific broth auto-induction media containing trace elements and supplemented with 8 g/L glycerol and antibiotics. Larger cultures were initiated with the overnight pre-culture and were allowed to grow at 37 ºC/220 rpm until OD_{600} reached 1. Next, the cultures were incubated overnight in an incubator shaker set at 18 ºC/180 rpm. The cells were collected by centrifugation and suspended in the lysis buffer. The purification of the produced proteins was usually done by two-step process, using nickel-affinity (Ni-affinity) chromatography and followed by size exclusion chromatography (Haikarainen *et al*, 2013b; Narwal *et al*, 2013a, 2013b, 2012a, 2012b; Venkannagari *et al*, 2013). In brief, Cells were lysed with lysozyme (2 µg/mL) and sonication, and solution was cleared by centrifugation. Supernatant was filtered through 0.45-µm filters and sample was loaded on HisTrap HP column (GE Healthcare) which was preequilibrated with binding buffer. Column was first washed with binding buffer and subsequently with washing buffer. Protein was eluted with an elution buffer having 250 mM imidazole and pooled fractions were loaded to size exclusion column (Hiprep 16/60 Sepharyl S-100 HR or Superdex S-200 10/30; GE Healthcare). Fractions from size exclusion chromatography were analyzed on sodium dodecyl sulfate-polyacrylamide gel electrophoresis (SDS-PAGE). Finally, protein preparations were divided to small aliquots and flash frozen using liquid N_2 into -70 ºC freezer.

3.3   Activity assay (I-V)

The fluorescence assay was adapted from the article by (Putt & Hergenrother, 2004). This assay measures the remaining substrate after the enzymatic reaction. The substrate consumption was quantified by converting the NAD^+ into a stable fluorescent condensation product upon treatment with acetone followed by heating in the acidic conditions. Reaction was carried out on black polypropylene U-shaped 96-well plate. After the enzymatic reaction, 20 µL of 20 % acetophenone and 20 µL of 2 M KOH were added. The plate was incubated at 4 ºC for 10 minutes and 90 µL formic acid was added after the incubation. The plate was transferred to 110 ºC oven for 5 minutes and read after 30 minutes. Later the assay was modified and plate was incubated at RT instead of 4 ºC, also step involving heating in the oven was omitted. Instead all the assay steps were performed at room temperature and plate was read 20 minutes after adding formic acid. Plate readers used were Varioskan flash (Thermo Fisher Scientific), Fluoroskan Ascent FL (labsystems) or Tecan plate reader (Infinite M1000 Pro and Infinite M200 Pro) at an excitation/emission wavelength of 355/460 nm using the filters and excitation/emission wavelength of 372/444 nm using the monochromators.

3.4   Optimization of assay conditions and assay repeatability (I, III)

Assay conditions were optimized by testing the effect of different buffer components on the enzymatic activity (**Fig. 3B** and **Table 1** in **I**). Different NAD^+ concentrations were also tested and their effect on the enzymatic reaction was examined. As compounds were stored in DMSO, therefore, DMSO tolerance of the assay was studied. Separate controls were used for each condition. The incubation time varied depending on the protein batch used but the aim was to reach approximately 25 % conversion in order to clearly see the effects of different reagents.

The assay performance was determined by measuring the maximal and minimum signal. To evaluate the positional effects during the incubation, well-to-well variations were measured. The plate-to-plate and day-to-day variations were also calculated by measuring two plates on the same day and two plates on different days. Assay repeatability was tested manually as well as using a pipetting robot (**Fig. 4A** and **Table 2** in **I**). Assay quality was evaluated using following statistical parameters: screening window coefficient (Z′ factor), signal-to-background (S/B) ratio (Zhang *et al*, 1999), signal to noise (S/N) ratio (Bollini *et al*, 2002), and coefficient of variation of the assay (CV_A) (Iversen *et al*, 2006). Z′ is a dimensionless term, which is used to evaluate, compare and validate bioassays. The acceptance criteria for Z′ is as follows; Excellent: Z′ > 0.5, Do-able: 0 < Z′ < 0.5, Yes/No assay: Z′= 0, Unacceptable: Z′ < 0 (Iversen *et al*, 2006; Zhang *et al*, 1999).

Final buffer used for TNKS1 and TNKS2 constructs containing ARTD and SAM domain was 50 mM Bis Tris propane, pH 7 supplemented with 0.01 % Troton X-100 and 0.5 mM TCEP. Whereas, buffer used for TNSK2 fragment containing only catalytic domain was 50 mM Bis Tris propane, pH 7 supplemented with 2 mM $NiCl_2$ and 1 mM TCEP.

3.5 Screening and potency measurements (I, III, IV, V)

Compounds were stored in DMSO at -20 ºC and they were diluted in the assay buffer prior to the experiments. Screening of the compounds was done in duplicates and separate controls were used for each compound. The final concentration of the compounds in the well was 10 µM or 1 µM. Hits were retested at 1 µM in triplicates to identify possible false positives.

The inhibitory potency of the hit compounds was measured in quadruplicates and in most of the cases; the experiment was repeated three times. Starting inhibitor concentrations were 100 µM or 10 µM and half log dilution was used. Reaction time was set to achieve less than 30 % conversion. Following terms are used in this thesis: Half maximal inhibitory concentration (IC_{50}-value) is defined as the concentration of compound required in order to inhibit 50 % activity of the enzyme, Half maximal effective concentration (EC_{50}-value) is the concentration of a compound where 50 % of its maximal effect could be observed. Potency is the measure of the activity of a drug in a biochemical assay and in this thesis sometimes the term 'potency' has been used to mention IC_{50}-value. Standard deviation (SD) is the measure of variation from the mean.

Ligand efficiency (LE) is defined as the binding affinity of a ligand in relation to number of non-hydrogen atoms and is calculated as LE = 1.4 ($-logIC_{50}/N$), where N is number of non-hydrogen atoms, and lipophilic efficiency (LipE) is a parameter used in drug design to link the potency and lipophilicity of compound and can be calculated as LipE = $pIC_{50} - logP$, where pIC_{50} is $-log_{10}(IC_{50})$ and *logP* is lipophilicity of the drug. IC_{50} curves were fitted with Graphpad Prism using sigmoidal dose response curve and four variables.

3.6 Western blot method (I, II)

A western blot method was used to confirm the results from the homogenous assay. Biotinylated NAD^+ (bioNAD$^+$) (1 µM) was used as the substrate in the enzymatic reaction. Laemmli buffer (Bio-rad) was added to stop the reaction and the sample was heated at 98 ºC for 5 minutes. Next, SDS-PAGE was run and gel was blotted onto the nitrocellulose membrane. Blocking was performed overnight with 1 % casein (Bio-Rad). Modified proteins were detected using streptavidin-conjugated horseradish peroxidase.

3.7 Crystallization and crystallography (II-V)

TNKS2 catalytic domain was used for crystallization. Chymotrypsin and 2mM TCEP were added to the purified TNKS2 protein solution and it was concentrated to 5.8 mg/mL. Chymotrypsin was added (one part to 100 parts by concentration of TNKS2), as protein was precipitating during centrifugation. Also, crystal form of chymotrypsin cleaved protein made it possible to soak inhibitors. Crystallization was done using sitting drop vapor diffusion method. The well solution contained 0.2 M Li_2SO_4, 0.1 M Tris-HCl, pH 8.5, and 24-26 % PEG 3350. Protein solution was mixed with the well solution in 2:1 or 1:1 ratio, and crystals appeared with in a week at 4 ºC. Pipetting robot (mosquito) was used in order to minimize the protein consumption and final size of the drops varied from 200 nanolitres to 300 nanolitres. Co-crystal structures were obtained by soaking the TNKS2 crystals in the well solutions containing the inhibitors. Compounds were soaked overnight except for EB-47 and rucaparib, for which the soaking time was three months. The inhibitor concentration used was in the range of 100 μM - 10 mM. Additionally, 250 mM NaCl was also added to the soaking solution in order to prevent the protein crystals from osmotic shock as there was salt present in the protein solution. Crystals were quickly dipped into a cryosolution supplemented with inhibitor, 250 mM NaCl and 20 % of glycerol, before flash freezing them in the liquid N_2 for data collection.

Diffraction data was collected at the synchrotrons situated in France (ESRF, Grenoble), UK (Diamond Light Source, Oxfordshire) or at the home source Bruker Microstar X-ray generator with PLATINUM CCD detector. Data were processed with XDS (Kabsch, 2010) and Proteum 2 suite (Bruker). Crystals belonged to the $C222_1$ or $P4_12_12$ space groups. The phases were determined with the molecular replacement program Molrep (Vagin & Teplyakov, 2010) from CCP4 program suite (Dodson *et al*, 1997). Apo-TNKS2 structure (PDB code: 3KR7) or TNKS2-nicotinamide co-crystal structure (PDB code: 3U9H) were used as search models. Water molecules and ligands were deleted from the models prior to molecular replacement. Refmac5 (Murshudov *et al*, 2011) from CCP4 program suite was used for molecular replacement and refinement. Manual building of the models was performed using Coot (Emsley & Cowtan, 2004). Validation of the results was performed using an online tool MolProbity from Duke University.

4   Results

The results will be summarized in this section, more detailed description of the results is available in the original articles (**I-V**).

4.1   Adaptation of an assay for screening the compounds

4.1.1   Protein expression and purification (I-V)

To determine the optimal media for TNKS1 protein expression, different culture media for *E. Coli* (Luria broth, $2 \times$ YT broth, super broth, Terrific broth) were tested in small scale (200 mL) using isopropyl-β-D-thiogalactoside (IPTG) induction or autoinduction methods. Protein fractions purified using Ni-affinity chromatography were run on SDS-PAGE to compare expression levels. Terrific Broth autoinduction media gave the best expression in comparison with other culture media. In case of TNKS1, Ni-affinity purification step yielded pure protein. However, gel filtration (GF) purification step increased the enzyme activity by four fold. Size exclusion chromatography revealed that the 37 kDa protein eluted as a high molecular weight (approx. 600 kDa) species in agreement with the reported multimerization. TNKS2 construct containing the catalytic domain was purified similarly using Ni-affinity chromatography and gel filtration methods (Narwal *et al*, 2012b). TNKS2 fragment containing the SAM domain in addition to the catalytic domain was purified in two steps using Ni-affinity and cation exchange chromatography (Haikarainen *et al*, 2013b; Narwal *et al*, 2013b; Venkannagari *et al*, 2013).

4.1.2   Assay optimization (I, III)

The best assay conditions for TNKS1 (containing SAM and ARTD domain) and TNKS2 (containing ARTD domain) were determined by testing various buffer types and components in the enzymatic assay. Different buffers were used to measure the protein activity in a pH range from 3.5 to 9. Based on the substrate conversion, protein was active over the pH range of 5-8 but the best activity was observed at pH 5.5 (**Fig. 3A** in **I**). However, pH 7 was selected for further optimization as this pH was close to the physiological pH and that also made it suitable for screening the compound libraries. Moreover, different buffers and buffer components such as divalent cations, reducing agents, detergents, salts, glycerol and BSA etc. were tested at pH 7 (**Table 1** in **I** and **Fig. 3B** in **I**). The final buffer used for TNKS1 was 50 mM Bis Tris propane supplemented with 0.01 % Triton-X-100 and 0.5 mM TCEP (Tris (2-carboxyethyl) phosphine) (**Fig. 3B** in **I**). The same buffer was used for TNKS2 fragment containing catalytic and SAM domains. In case of TNKS2 fragment containing only catalytic domain, 50 mM Bis Tris propane supplemented with 2 mM $NiCl_2$ and 1 mM TCEP (Tris (2-carboxyethyl) phosphine) was found to be the best for activity. The TNKS1 automodification activity was protein concentration and incubation time

dependent. However, diluting it to lower concentrations led to loss of the activity (**Fig. 3C,D** in **I**). The rate of substrate conversion was also found to be linear with time when the conversion was lower than 50 % (**Fig. 3D** in **I**).

4.1.3 Assay validation (I, III)

In order to validate the assay, plates containing the maximal and minimal signals were analyzed. The results showed that the signals followed binomial distribution (**Fig. 4A** in **I**). A good dynamic signal range was observed and the qualitative parameters (S/B, S/N and CV_A) were calculated (**Table 2** in **I** and **Table 1** in **III**). Z´ value for the manual assay for both TNKS1 and TNKS2 was 0.72. Thus, Z´ value along with the calculated parameters clearly indicated the suitability of the assay for the compound screenings. Different NAD^+ concentrations were tested for TNKS1 and 500 nM was used as it gave the best results (Z´ > 0.7). However, even at lower NAD^+ concentrations, assay was found to be useful (Z´ > 0.6). Assay performance was not affected when conducted using the automated system (**Fig. 4A** and **Table 2** in **I**). As compound libraries were stored in DMSO, a DMSO tolerance test of the assay was performed. The assay showed tolerance up to 2 % of the DMSO in case of TNKS1 and up to 3 % in case of TNKS2 without any significant effect on the enzyme activity, making it appropriate to test compounds even at the concentrations over 100 μM.

4.1.4 Validatory Screening and potency measurements (I)

A chemical library consisting of 142 natural products was screened at 10 μM concentration (**Fig. 5A** in **I**). Separate controls containing the compounds and NAD^+ were used for each compound. The hit limit was set at 2 × SD from the controls and nine hit compounds were identified. Five of them were found to be flavone derivatives (apigenin, luteolin, myricetin, alpha-napthoflavone, and flavone) (**Fig. 5B** in **I**). Flavone had been identified earlier also in a yeast based assay (Yashiroda *et al*, 2010). The best TNKS1 inhibitor was flavone (**1** in **Table 4**) followed by luteolin (**3** in **Table 4**), apigenin (**2** in **Table 4**) and isopropyl gallate. Although one more gallate, gallotannin showed inhibition, other gallates present in the chemical library were not able to inhibit TNKS1. A western blot using $bioNAD^+$ as a substrate was also used to complement the fluorescence assay results. The western blot results showed that all the compounds were able to inhibit at 10 μM, while flavone stood out as the best inhibitor (**1** in **Table 4**). Known potent tankyrase inhibitors XAV939 and IWR-1 were used as controls, and they completely inhibited the enzyme activity. Potency measurements were conducted for four most potent hits flavone, apigenin, luteolin and isopropyl gallate against TNKS1, ARTD1 and ARTD2. Luteolin (**3** in **Table 4**) did not show selectivity towards tankyrases, while others were found to be selective towards TNKS1.

4.2 Identifications of flavones as potent and selective tankyrase inhibitors (III, IV)

Flavones were found to be the best tankyrase inhibitors during the validatory screening using natural product library (Narwal *et al*, 2012a). Flavone was the most potent hit in the screened natural product library and other flavones such as apigenin and luteolin were not very potent, but still showed selectivity towards tankyrases over ARTD1. This suggested that flavonoids could contain novel scaffolds selectively inhibiting tankyrases.

4.2.1 Screening of the flavonoids library and binding mode of flavones (III)

Flavonoids contain a benzene ring condensed with a pyran or pyrone ring which is further attached to a phenyl group. A nature-inspired flavonoid library containing 500 compounds was screened using TNKS2 catalytic domain. Compound library was screened in duplicates at 1 µM concentration and the hit limit was set to 60 % activity in order to identify compounds of equal or better potency compared to the base compound flavone (**1** in **Table 4)**. Ten compounds displayed inhibition against TNKS2, and were re-tested to confirm the results. Finally, seven compounds were identified as inhibitors. Interestingly, all the hits contained the common flavone scaffold. Inhibitor potencies were measured for TNKS1, TNKS2 and ARTD1. Results (**Table 4**) showed that IC_{50}-values were in the range of 0.047 µM – 3.1 µM for TNKS1. Compound **2** despite of having potency value in µM range showed selectivity (33-folds) towards tankyrases compared to ARTD1. In addition, compound **5** displayed even higher selectivity (over 200-folds) towards tankyrases (**Table 4**).
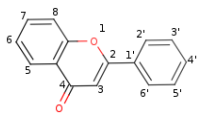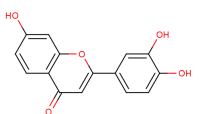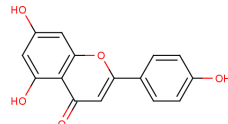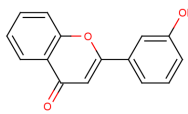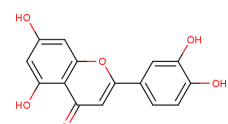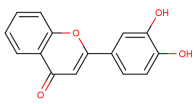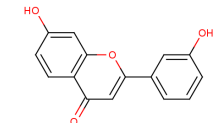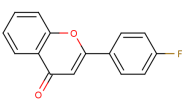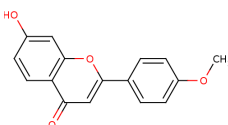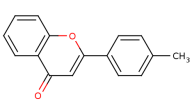
The crystal structure of TNKS2 in complex with flavone (**1** in **Table 4**) showed that it binds to the nicotinamide site of the binding cavity. The oxygen of the benzopyran-4-one forms hydrogen bonds with the main chain amide of Gly1032 and hydroxyl of Ser1068. The pyran ring of flavone forms π-π interactions with Tyr1071. In contrast to other typical ARTD inhibitors, flavone contains a carbon at position 3 instead of amide, which was situated at a hydrogen bond distance from the main chain carbonyl of Gly1032.

The above mentioned interactions were shared by most of the flavone derivatives with some exceptions. Compound **2** (4′, 5, 7-trihydroxyflavone) (IC_{50} = 3.1 µM) and **3** (3′,4′,5,7-tetrahydroxyflavone) (IC_{50} = 2.4 µM) (**Table 4**) had additional hydroxyl groups attached to the flavone scaffold. The hydroxyl at position 5 formed a nonoptimal hydrogen bond with the Ser1068 hydroxyl. However, the 4-hydroxyl was pushed further away, and did not make any interaction with Ser1068. The co-crystal structures of TNKS2 in complex with **2** and **3** revealed that Ser1068 exhibited two conformations. Other hydroxyl groups made hydrogen bonds with the protein and water molecules (**Fig. 5b,c** in **III**). The

hydroxyl at position 7 in compounds **2**; **3**; **4** (3´,7-dihydroxyflavone) (IC_{50} = 0.28 µM); **5** (7-hydroxy, 4´-methoxyflavone); (IC_{50} = 0.56 µM); and **6** (3´,4´, 7-trihydroxyflavone) (IC_{50} = 0.63 µM); formed hydrogen bonds with the catalytic Glu1138 *via* their 7-hydroxyl group (**Fig. 5a-f** in **III**) (**Table 4**).

The compounds containing 3´-hydroxyl group such as **4**, **6, 7** (3´-hydroxyflavone) and **8** (3´,4´- dihydroxyflavone) (**Table 4**) were hydrogen bonded to water molecule connecting the compound with the His1031 and Ser1033. Compounds **5**, **9** and **10** contained methoxy, fluorine and a methyl substituent, respectively at position 4´ (**Table 4**). These substituents mostly formed the hydrophobic interactions with Pro1034 and Phe1035. Notably, these three compounds were also selective toward TNKS1 over TNKS2.

Table 4. Chemical structure of Flavones inhibiting tankyrases. IC_{50}-values are indicated against TNKS1, TNKS2 and ARTD1.

	Structure	IC_{50}		Structure	IC_{50}
1		TNKS1 330 nM TNKS2 140 nM ARTD1 1.4 µM	6		TNKS1 630 nM TNKS2 870 nM ARTD1 7.5 µM
2		TNKS1 3.1 µM TNKS2 2.9 µM ARTD1 ~100 µM	7		TNKS1 310 nM TNKS2 310 nM ARTD1 2.4 µM
3		TNKS1 2.4 µM TNKS2 1.1 µM ARTD1 4.2 µM	8		TNKS1 230 nM TNKS2 170 nM ARTD1 1.3 µM
4		TNKS1 280 nM TNKS2 620 nM ARTD1 9.5 µM	9		TNKS1 280 nM TNKS2 1.1 µM ARTD1 9.9 µM
5		TNKS1 560 nM TNKS2 450 nM ARTD1 >100 µM	10		TNKS1 47 nM TNKS2 1.1 µM ARTD1 25 µM

4.2.2 Screening of the flavones with single substitutions and co-crystal structures (IV)

Based on the aforementioned results, we decided to screen commercially available flavones with single substitutions to identify the features required for
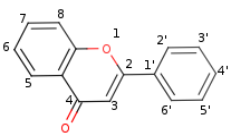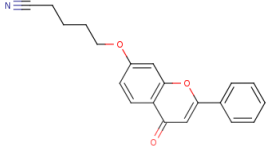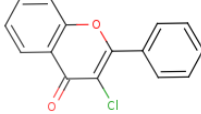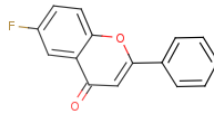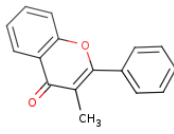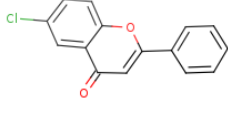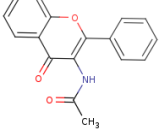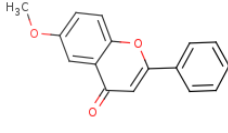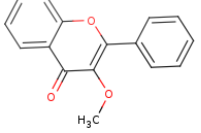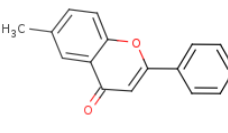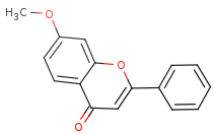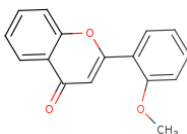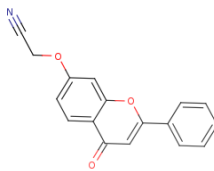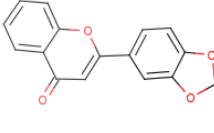
the potency and selectivity (**Table 5a, 5b**). This screening was performed using TNKS1 and complex crystal structures with the potent compounds were solved using TNKS2 catalytic domain. Biochemical assay results showed that the substitutions to other than 4´-position, abolished the compound inhibitory activity in most of the cases with some exceptions (**Table 5a**). Co-crystal structures of TNKS2 were solved in complex with potent inhibitors. The structures were solved at 1.7 Å - 2.3 Å resolution (**Supplementary Table 1** in **IV**). The crystal structures explained the potency values of the compounds. Introduction of hydrophobic or halogen atoms to position 3 abolished the activity of the compounds (**Table 5a**). Analysis of crystal structures showed that compounds **2-5** containing substitutions at position 3 cannot inhibit because there is no space to accommodate the substitution and the compounds would clash with Gly1032 (**Fig. 4.** in **IV**). Similarly introducing the substituents to position 7 (compounds **6-8**) (**Table 5a**) would lead to clashing with the catalytic Glu1138. Compounds **11** and **12** contained methoxy and methyl groups to position 6. These groups will again clash with the catalytic Glu1138 and also with the main chain of Phe1061. Likewise, introducing the methoxy group (compound **13**) to position 2´ or 6´ (**Table 5a**) would cause clashes with the side chain of His1031 and with Gly1032 or Tyr1050. These compounds were not able to inhibit even at 10 μM concentration. Halogen substitutions to position 6 such as in compounds **9** and **10** were tolerated and the potencies (**9**, IC_{50} = 210 nM and **10**, IC_{50} = 595 nM) (**Table 5a**) were comparable to the base compound.

Compound **9** contained the fluorine atom at position 6, this fluorine didn't form any hydrogen bonds, and the compound had the same interaction as the base compound **1**. However, fluorine was close to the hydrophobic parts of the side chains of Glu1138, Lys1067, Ala1064 and Phe1061. The analysis of complex crystal structure showed that there was enough space to accommodate this substitution (**Fig. 4b** in **IV**) and that is why compound **9** was able to inhibit tankyrases.

Compound **10** (**Fig. 4c** in **IV**) contained chlorine in position 6, and the larger size of chlorine might be reason for its lower potency compared to compound **9**. Introduction of hydrophobic groups to position 6 led to only weak inhibition. The substitution of dioxolane ring fused with phenyl group in compound **14** at position 3´ and 4´ was well tolerated, and has an IC_{50}-value of 360 nM comparable to flavone (**Table 5a**). This modification was tolerated as there is space in the binding cavity to accommodate this (**Fig. 4d** in **IV**).

In contrast, modifications to position 4´ improved the potency, and in some of the cases also led to the better selectivity in comparison to the base compound (**Table 5b**). The substitutions of halogens (compounds **15-17**) (**Table 5b**) resulted in variable potency (**15**, IC_{50} = 700 nM; **16**, IC_{50} = 233 nM; **17**, IC_{50} = 313 nM) depending on their sizes and their interactions with the neighboring hydrophobic residues Pro1034 and Phe1035 (**Fig. 5a,b,c** in **IV**). However, there was no improvement in the potency compared to **1**.
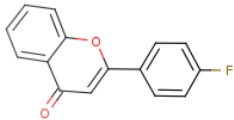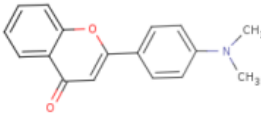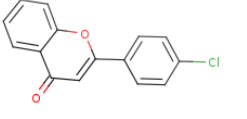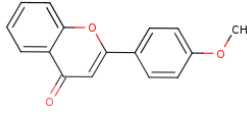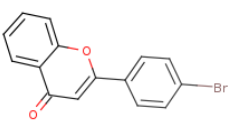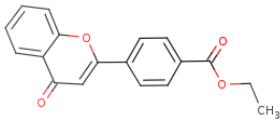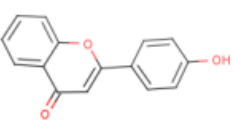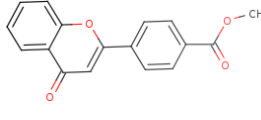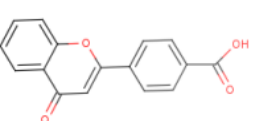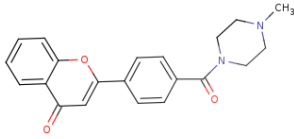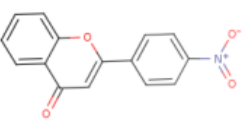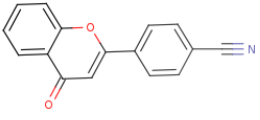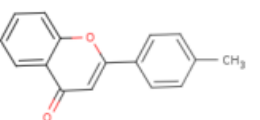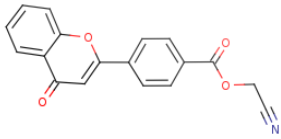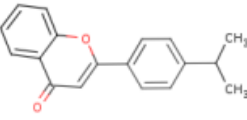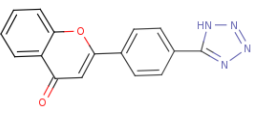
Table 5a. Evaluation of flavone derivatives as tankyrase inhibitors. IC_{50}-values were measured for **1**, **9**, **10** and **14** against TNKS1

	Structure	IC_{50}		Structure	IC_{50}
1		330 nM	**8**		>10 µM
2		>10 µM	**9**		210 nM
3		>10 µM	**10**		595 nM
4		>10 µM	**11**		>10 µM
5		>10 µM	**12**		>10 µM
6		~5 µM	**13**		>10 µM
7		>10 µM	**14**		360 nM

Compounds **18** (IC_{50} = 788 nM) and **19** (IC_{50} = 850 nM) contained a hydroxyl group and a carboxyl group, respectively. These compounds were not potent, because they were surrounded by the hydrophobic residues Pro1034 and Phe1035 and had non-favorable interactions (**Fig. 5d,e** in **IV**). However, introduction of nitro group (compound **20**) improved the potency (IC_{50} = 66 nM) by forming the hydrogen bonds with Ala1049 and Ile1051 through one bridged water molecule (**Fig. 5f**. in **IV**). Compounds **21** (methyl) and **22** (isopropyl) (**Fig. 8**) improved

the potency a lot with the IC_{50}-values of 47 nM and 6 nM (**Table 5b**). This improvement was because of their efficient hydrophobic interactions with Pro1034 and Phe1035 (**Fig. 5g,h** in **IV**).

Table 5b. Evaluation of flavone derivatives as tankyrase inhibitors. IC_{50}-values are shown against TNKS1

	Structure	IC_{50}		Structure	IC_{50}
15		700 nM	23		67 nM
16		233 nM	24		71 nM
17		313 nM	25		272 nM
18		788 nM	26		162 nM
19		850 nM	27		146 nM
20		66 nM	28		145 nM
21		47 nM	29		7 nM
22		6 nM	30		114 nM
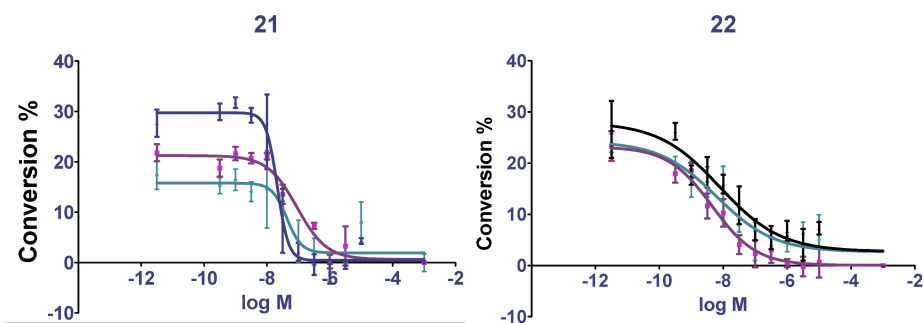
Figure 7. IC_{50}-value measurement of the compounds 21 and 22 for TNKS1. Log of molar concentration of inhibitor (log M) is plotted on x-axis and conversion % is plotted on y-axis. Standard deviation is shown for each point. Curves were fitted with Graphpad Prism using sigmoidal dose response curve and four variables.

Dimethyl amine substitution in **23** showed improvement in the potency ($IC_{50} = 67$ nM) compared to the base compound **1**. This was because of the additional hydrogen bonding with the water network (**Fig. 5i** in **IV**). Compound **24**, carrying a methoxy group, ($IC_{50} = 71$ nM) (**Fig. 5j** in **IV**) displayed improvement in selectivity due to hydrophobic interactions similar to **21** and **22**.

Substituting the 4´-position with ethyl methanoate (**25,** $IC_{50} = 271$ nM) and methyl methanoate (**26,** $IC_{50} = 162$ nM) had similar hydrophobic interactions and hydrogen bonds with the protein molecule (**Table 5b**) (**Fig. 5k,l** in **IV**). The co-crystal structure of TNKS2 in complex with compound **27** (methylpiperazine-1-carbonyl) ($IC_{50} = 146$ nM) showed that the D-loop was moved to accommodate the inhibitor. The core of the compound was rotated approximately 5º towards Tyr1071. The residues 1046-1051 lining the D-loop were moved approximately 0.9 Å in order to accommodate the large substituent. This movement has loosened the packing between the D-loop residues and active site helix 1059-1062, and also His1048 was rotated disrupting the hydrogen bond betwee+n His1048 and Asp1045 (**Fig. 5m** in **IV**).

Compound **28** (**Table 5b)** contained a cyano group and in spite of having a better potency ($IC_{50} = 145$ nM) compared to the base compound, it didn't make any additional interactions with the protein molecule (**Fig. 5n** in **IV**). In contrast to the other compounds, **29** containing the cyanomethyl acetate substituent was the only inhibitor that formed the direct hydrogen bond with the protein molecule (**Fig. 5o** in **IV**). This additional hydrogen bond accounted for the very low IC_{50}-value of 7 nM of this compound. Compound **30** (**Table 5b**) had a tetrazol substitution and it formed an additional hydrogen bond with a water molecule (**Fig. 5p** in **IV**) and displayed an IC_{50}-value of 114 nM (**Table 5b**).
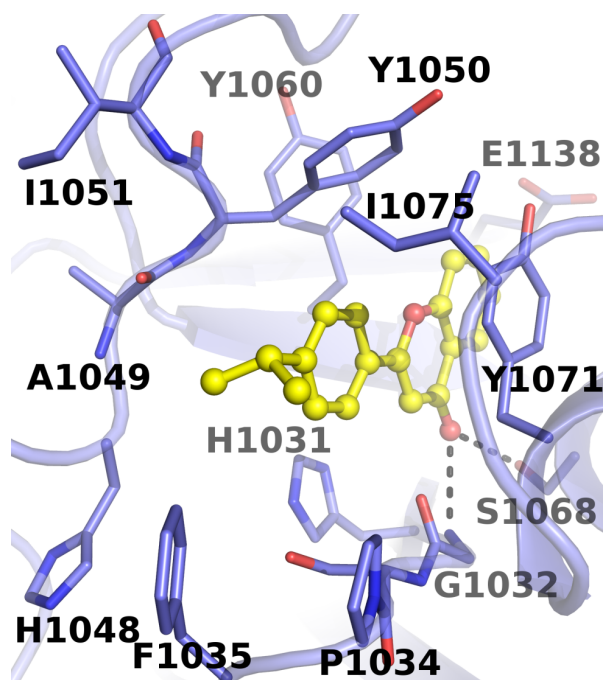
Figure 8. Binding mode of compound **22** (in yellow) with TNKS2 catalytic domain (in blue). Hydrogen bonds between the compound and protein molecule residues are presented as black dashed line.

4.2.3   Inhibition of Wnt signaling and profiling of the inhibitors (IV)

The compounds with an IC_{50}-value cut-off of 200 nM were further tested in a cell-based assay using SuperTopFlash (STF) TCF-reporter plasmid (**Fig. 1** in **IV**). Ten compounds were tested at three different concentrations. Seven compounds showed inhibition at 5 µM, but at 200 nM only compound **22** showed inhibition. (**Fig. 1** in **IV**). Thus, the efficacy of **22** in cell-based assay and also in biochemical assay made it the best inhibitor in the library tested.

To determine the selectivity of the hit compounds, they were profiled against a panel of ARTD superfamily members (**Fig. 2** in **IV**). Results revealed that most of the compounds did not inhibit other ARTD enzymes at 1 µM concentration. Compound **22** was the most potent and also the most selective compound, as it displayed very low potency for other isoenzymes. Selectivity of the best compounds was confirmed by measuring the IC_{50}-values against ARTD1 (**22,** IC_{50} = 19.1 µM), ARTD2 (**22,** IC_{50} = 34.9 µM), TNKS1 (**22,** IC_{50} = 6 nM) and TNKS2 (**22,** IC_{50} = 72 nM) using the biochemical assay, and XAV939 was used as a control compound (**Table 3** in **IV**). Analysis of the potency values showed that **22** was the most potent and selective compound. Compound **22** improved the

selectivity in comparison to XAV939 and also maintained the single digit nanomolar potency against TNKS1.

4.3   Inhibitor binding to adenosine site (II)

4.3.1   Co-crystal structure of TNKS2 catalytic domain in complex with IWR-1

The co-crystal structure of TNKS2 containing IWR-1 (**Fig. 3c** in **II**) was determined using protein X-ray crystallography. Unlike all other known ARTD inhibitors at that time, IWR-1 (**Fig. 6**) did not utilize the traditional nicotinamide binding site and was rather bound to the adenosine site (**Fig. 3c** in **II**). The solved crystal structure showed that the compound induced movement of the D-loop, which otherwise is in the closed conformation in the apo structure. Chemically IWR-1 structure could be divided into three parts: amide, spacer and norbornyl region (**Fig. 6**). The carbonyl oxygen of the amide region formed hydrogen bond with the amide of the Asp1045. Amide region in the inhibitor contained a quinolone moiety that was situated between the hydrophobic face of the helix 1035-1042 and His 1048, that would have clashed with the amide region if not moved out of the cavity.

Spacer region of IWR-1 was present in between the reorganized D-loop and in the vicinity of hydrophobic region formed by His1031, Phe1044 and Ile1059. The carbonyl oxygens of the norbornyl region formed two hydrogen bonds with the backbone amides of Tyr1050 and Tyr1060. The norbornyl region was located in the middle of three tyrosines (Tyr1050, Tyr1060 and Tyr1071) and had nonpolar interactions with them (**Fig. 3c** in **II**). All of the tyrosines adopted a different conformation in comparison to other known crystal structures. The Tyr1050 was moved 5 Å away from the cleft and formed nonpolar interactions with IWR-1 and Ile1075. The Tyr1060 side chain was moved 1 Å towards IWR-1. Tyr1071 showed a rotation of 51º in order to interact with the compound and this closed the nicotinamide-binding site. The catalytic Glu1138 also adopted a slightly different conformation in comparison to nicotinamide bound structure (**Fig. 3c** in **II**).

4.3.2   Structure-activity relationship studies of IWR-1 analogues

Prior to this contribution, a structure-activity relationship study of IWR analogues using the cell based assays was published (Lu *et al*, 2009). In that study, it was suggested that all three regions of the compound are important for potency. At that time the molecular target of IWR-1 (**Fig. 6**) was unknown and now with the help of TNKS2-IWR-1 complex crystal structure, some of the effects in the cells could be explained. In the crystal structure, the movement of His1048 and rotation of Phe1035 led to the formation of a new cavity which is occupied by the quinoline moiety of the amide region (**Fig. 5a** in **II**). Quinoline

ring was very critical for the potency and substitution of quinoline ring with smaller aromatic groups such as phenyl, benzyl, and pyridyl groups have led to almost complete loss of activity ($EC_{50} > 20$ µM). However, the phenyl derivatives with halogen substitution at position 4 ($EC_{50} \sim 2.6$ µM) and 4-pyridyl-methyl derivatives ($EC_{50} = 10$ µM) improved the potency. These substitutions might form favorable interactions with Lys1042 and direct the compound to bind tightly to the protein molecule (**Fig. 3c** in **II**). Trans-(2-methoxy) cyclohexyl and 2-methoxyphenyl analogues showed improved potency of 2 µM and 1 µM respectively. This might be because of their hydrophobic interactions with the α-helix 1035-1042 (**Fig. 4** in **II**). Notably, N-methyl derivatives were inactive because they would not allow the conformation of the compound observed in the crystal structure.

Spacer region forms hydrophobic interactions with the side chains of the protein molecule (**Fig. 3c** in **II**). The length of the spacer region was found to be more critical in comparison to its aromaticity. The addition of just one atom inactivated the compound completely, and saturated analogue showed reasonable potency (0.2 µM). Small substitutions to position 3 (**Fig. 6**) in the spacer region were tolerated because of the flexibility of D-loop. However, substituents at position 2 (**Fig. 6**) completely abolished the activity. Saturation of norbornyl region did not affect the potency of the inhibitor, while exo-IWR-1 (exo-isomer of the compound) was less potent and was effective only at higher concentration. This might be because exo-IWR-1 is less complementary to the binding site.

4.3.3   IWR-1 selectivity

IWR-1 was identified as a very selective tankyrase inhibitor. It has IC_{50}-values of 131 nM and 56 nM for TNKS1 and TNKS2, respectively, compared to an approximate IC_{50}-value of more than 18.7 µM for ARTD1 and ARDT2 (Huang *et al*, 2009). To confirm the results we measured the effect of IWR-1 on ARTD1 and ARTD2, and the results showed that IC_{50}-value for ARTD1 and ARTD2 would be 100 µM and 35 µM, respectively. Therefore, IWR-1 was 600-fold selective towards tankyrases compared to ARTD1 and ARTD2. These results were verified in another contribution (Haikarainen *et al*, 2013a). Superposing the ARTD1 crystal structure on the TNKS2-IWR-1 structure elucidated the features that could explain the IWR-1 selectivity (**Fig. 5b** in **II**). In the TNKS2 complex structure with IWR-1, Tyr1060 and Asp1045 of TNKS2 formed hydrogen bonds with the compound. In case of ARTD1, these amino acids are replaced by Tyr896 and Asp766. Asp766 could form a hydrogen bond with the carbonyl of the norbornyl region, if it is protonated. The norbornyl of the compound was surrounded by three tyrosines in TNKS2, whereas in ARTD1 only two of them (Tyr889 as Tyr1050 and Tyr896 as Tyr1060) were conserved. Furthermore, Ile1075 and zinc binding motif are absent in ARTD1, and Ile1075 is replaced by a negatively charged chain of Gln763 of regulatory domain at this position.

Major differences between TNKS2 and ARTD1 were noticed at the quinoline-binding site. The hydrophobic residues Phe1035 and Phe1044 are not conserved in ARTD1, and Phe1035 is completely absent. In ARTD1, binding site is surrounded by more polar amino acids compared to TNKS2. The quinoline of IWR-1 would clash with the salt bridge formed by Arg878 and Asp770 of ARTD1 regulatory domain. Also, the stacking interaction of His1048 with quinoline is not conserved in ARTD1 (**Fig. 5b** in **II**). The structural differences between the catalytic domains of TNKS2 and ARTD1 along with the novel features of IWR-1 made it a good compound for further development as a selective tankyrase inhibitor.

4.4   Characterization of known ARTD inhibitors (V)

In order to evaluate known ARTD inhibitors as tankyrase inhibitors, they were screened against TNKS1 using fluorescence-based activity assay and potencies were measured for the hit compounds. Finally, co-crystal structures were solved using protein X-ray crystallography and structure-activity relationship was established.

4.4.1   Screening of the inhibitors and potency measurements

Screening of the known ARTD inhibitors was conducted at 10 µM concentration and 14 compounds out of 32 showed more than 50 % inhibition (**Fig. 1** in **V**). In order to confirm the results and to identify the most potent hits, the small chemical library was re-screened at 500 nM. Nine compounds still displayed more than 20 % inhibition and these compounds were chosen for further characterization. All of the hits, except IWR-1, contained the nicotinamide motif. Five of these compounds were already reported as tankyrase inhibitors and had been characterized with protein X-ray crystallography, these compounds included **17** (PJ-34; TNKS1, IC_{50} = 570 nM) (Kirby *et al*, 2012; Wahlberg *et al*, 2012), **21** (Olaparib; TNKS1, IC_{50} = 1500 nM) (Menear *et al*, 2008; Narwal *et al*, 2012b), **23** (XAV939; TNKS1, IC_{50} = 11 nM) (Huang *et al*, 2009; Karlberg *et al*, 2010), **26** (IWR-1; TNKS1, IC_{50} = 130 nM) (Narwal *et al*, 2012b), and **32** (flavone; IC_{50} = 330 nM) (Narwal *et al*, 2013a, 2012a; Yashiroda *et al*, 2010).

Therefore, the binding mode of additional four compounds was studied using protein X-ray crystallography. These compounds were **10** (EB-47) (Jagtap *et al*, 2004), **16** (Phenanthridinone) (Banasik *et al*, 1992), **18** (TIQ-A) (Chiarugi *et al*, 2003), and **29** (Rucaparib) (Thomas *et al*, 2007) (**Fig. 9**). In a previously reported structure, PJ-34 was bound to both the sites in binding cavity; therefore, PJ-34 was also selected for the structural studies. PJ-34 (Compound **17**) is also a phenanthridinone and TIQ-A (Compound **18**) structure is also similar to compound **16** and **17** with three aromatic rings fused together (**Fig. 9**). Rucaparib contains three rings with one seven membered non-aromatic ring, and also had a large (methylaminomethyl) phenyl substituent. EB-47 was designed to mimic

NAD$^+$; it has a nicotinamide part attached to the adenosine part with a linker replacing the ribose-diphosphate (**Fig. 9**).
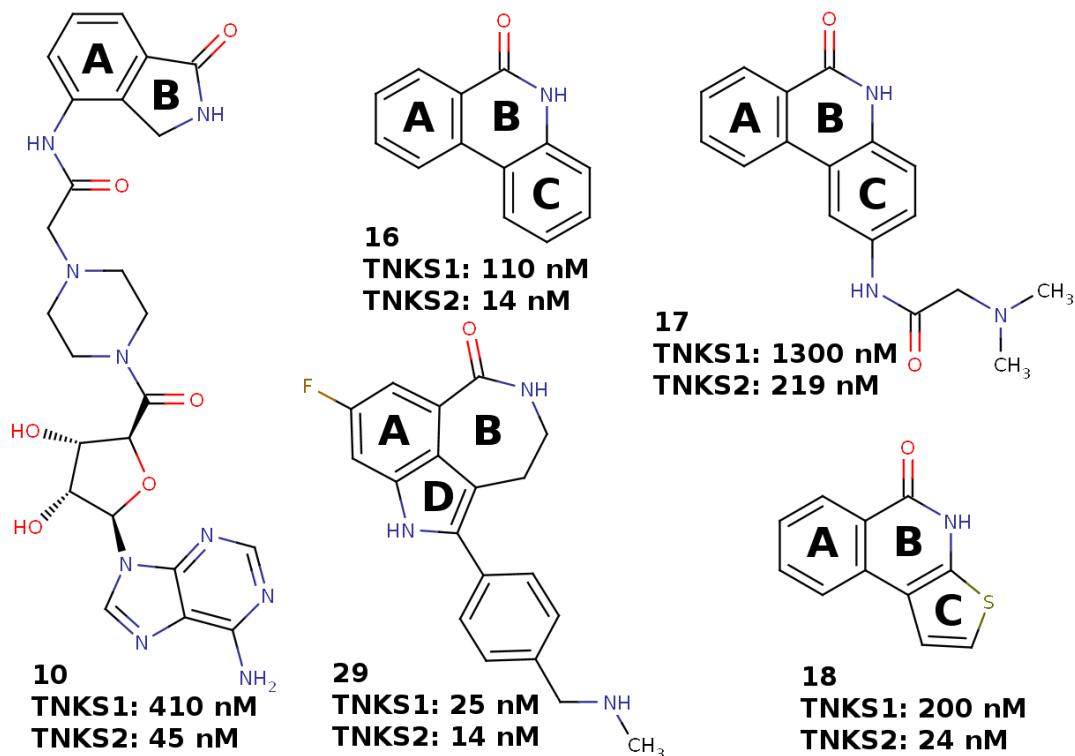
Figure 9. Chemical structures of the hit compounds; EB-47 (**10**), Phenathridinone (**16**), PJ-34 (**17**), TIQ-A (**18**), and Rucaparib (**29**) are presented. IC$_{50}$-values are indicated for TNKS1 and TNKS2

Compounds **16** and **18** displayed IC$_{50}$-values of 110 and 200 nM, respectively. Though, **17**, which is a derivative of **16** showed lower potency of 1300 nM. **10** showed a potency of 410 nM. **29** emerged as the best scaffold for inhibiting TNKS1 among hits with an IC$_{50}$-value of 25 nM (**Fig. 9**). However, **10** and **29**, both displayed selectivity towards ARTD1 over TNKS1 (**Table 1** in **V**). The potencies of these five compounds were also measured with ARTD1 and TNKS2. Surprisingly, these compounds were selective towards TNKS2 over TNKS1 (**Fig. 9**).

4.4.2 Binding modes of the compounds

Binding mode of **10** (EB-47) will be discussed in detail in the section 4.5. Other compounds will be discussed here.

4.4.2.1 Binding modes of Phenanthridinone (16) and TIQ-A (18)

16 and **18** (**Fig. 9**) make known interactions with the protein molecule (**Fig. 2a,b** in **V**). They formed hydrogen bonds with Gly1032 and Ser1068 and the characteristic π-π interactions with Tyr1071. These inhibitors form hydrophobic interactions with Tyr1060 and Lys1067, and aromatic C-ring also have hydrophobic interactions with Tyr1050 and Ile1075. Both of the co-crystal structures were very similar and the difference in potency might come from better interactions of the six membered ring of the **16** (**Fig. 9**) Tyr1050 and Ile1075 are not conserved in ARTD1 that could explain slight selectivity towards TNKS1 over ARTD1.

4.4.2.2 Binding mode of PJ-34 (17)

Binding mode of **17** was very similar to the binding modes of **16** and **18** (**Fig. 2c** in **V**). The compounds made all the characteristic interactions of general ARTD inhibitors. However, the presence of long dimethylamino acetamide tail in PJ-34 (**17**) caused the opening of the D-loop in the co-crystal structure as otherwise the tail would have clashed with the Tyr1050. The D-loop was opened up and it did not make any stable interactions with the compound. In addition, the tail of the compound avoids contact with Tyr1050, and also had poor electron density in the crystal structure (**Fig. 2c** in **V**). Tyr1060 also rotated approximately 15 degrees towards the compound compared to the TNKS2-**16** co-crystal structure. The hydrogen bond length of the amide of **17** with the carbonyl of Gly1032 was 2.9 Å (compared to 2.7 Å in both **16** and **18** structures). Previously, a complex crystal structure of TNKS2 was reported with **17** that had two molecules of the compound binding to the protein molecule (Kirby *et al*, 2012). In contrary, we observed only one molecule binding to the nicotinamide site.

4.4.2.3 Binding mode of Rucaparib (29)

Compound **29** is a large inhibitor and possesses a molecular weight of 323 Da (**Fig. 9**). It is an optimized ARTD1 inhibitor containing a nicotinamide-like motif fused with a seven membered B-ring (**Fig. 1** in **V**). **29** also forms known interactions at the nicotinamide site. Like **17**, the hydrogen bond distance with the Gly1032 was 2.9 Å. The fluorine atom of the compound was interacting with the hydrophobic regions of the catalytic Glu1138 and Ala1068 (**Fig. 2d** in **V**). The amide of the D-ring forms a hydrogen bond with the water molecule which is further interacting with a network of water molecules. Like the tail of **17**, (methylaminomethyl) phenyl substituent also extends from the nicotinamide site and causes changes in the active site. D-loop opened up and was completely disordered in the crystal structure (**Fig. 2d** in **V**). Large phenyl group also caused changes in the structure by rotating Tyr1060 and Tyr1071 15 degrees and 30 degrees, respectively. This rotation made Tyr1071 parallel to the aromatic D-ring. In addition, phenyl group also changed the conformation of Ile1075 (**Fig. 2d** in **V**).

Although, binding of **29** also disordered the D-loop, the additional interactions made by **29** with its tricyclic core and efficient stacking with the hydrophobic residues at the active site made it highly potent TNKS inhibitor.

4.5 Substrate Binding (II, V)

There is no substrate bound structure available; therefore, we soaked NAD^+ and one NAD^+ mimic compound (EB-47) in order to understand the molecular interactions between the substrate and TNKS2 catalytic domain.

4.5.1 Co-crystal structure of TNKS2 catalytic domain in complex with nicotinamide (II)

In order to solve the NAD^+ bound crystal structure, TNKS2 crystals were soaked in high concentrations (10 mM) of the substrate. However, only nicotinamide was found to be bound to the TNKS2 protein crystals instead of NAD^+. Nicotinamide, as expected, was binding to the nicotinamide site in the crystal structure. The carboxamide was hydrogen bonded to the Gly1032 and Ser1068, and nicotinamide also had π-π interactions with Tyr1071 (**Fig. 2a** in **II**). The stacking is not efficient because aromatic ring was situated at an angle of 39 degrees with respect to the plane of Tyr1071. In addition, nicotinamide formed hydrogen bonds with the water molecules present next to the conserved HYE triad made by His1031, Tyr1071 and Glu1138 (**Fig. 2a** in **II**). The TNKS2 protein used in the structure determination was treated with chymotrypsin, therefore this result showed that even chymotrypsin cleaved protein could catalyze automodification reaction and it was also verified with western blot (**Fig. 2b** in **II**).

4.5.2 Co-crystal structure of TNKS2 catalytic domain in complex with EB-47 (V)

EB-47 (**10**) is a known ARTD1 inhibitor that was designed to mimic the ARTDs substrate NAD^+ (Jagtap *et al*, 2004). The chemical structure of **10** consists of a nicotinamide region attached to the adenosine moiety with a linker replacing ribose-diphosphate (**Fig. 10a**). In the crystal structure, **10** binds to the NAD^+ binding channel, and extends from the nicotinamide binding site to the adenosine binding site. Isoindolinone moiety of the inhibitor bound to the nicotinamide site and formed hydrogen bonds with the Gly1032 and Ser1068 (**Fig. 10a**). Compound binding caused the opening of the D-loop, and unlike in the **17** and **29** co-crystal structures, the loop was visible in the crystal structure. Tyr1050 was moved out of the binding cavity. Carbonyl of the linker interacted with the backbone of Tyr1060 through water molecules (**Fig. 10a**). Other interactions made by linkers are hydrophobic in nature. Hydroxyls from the ribose moiety formed hydrogen bonds with His1031 and Ser1033.
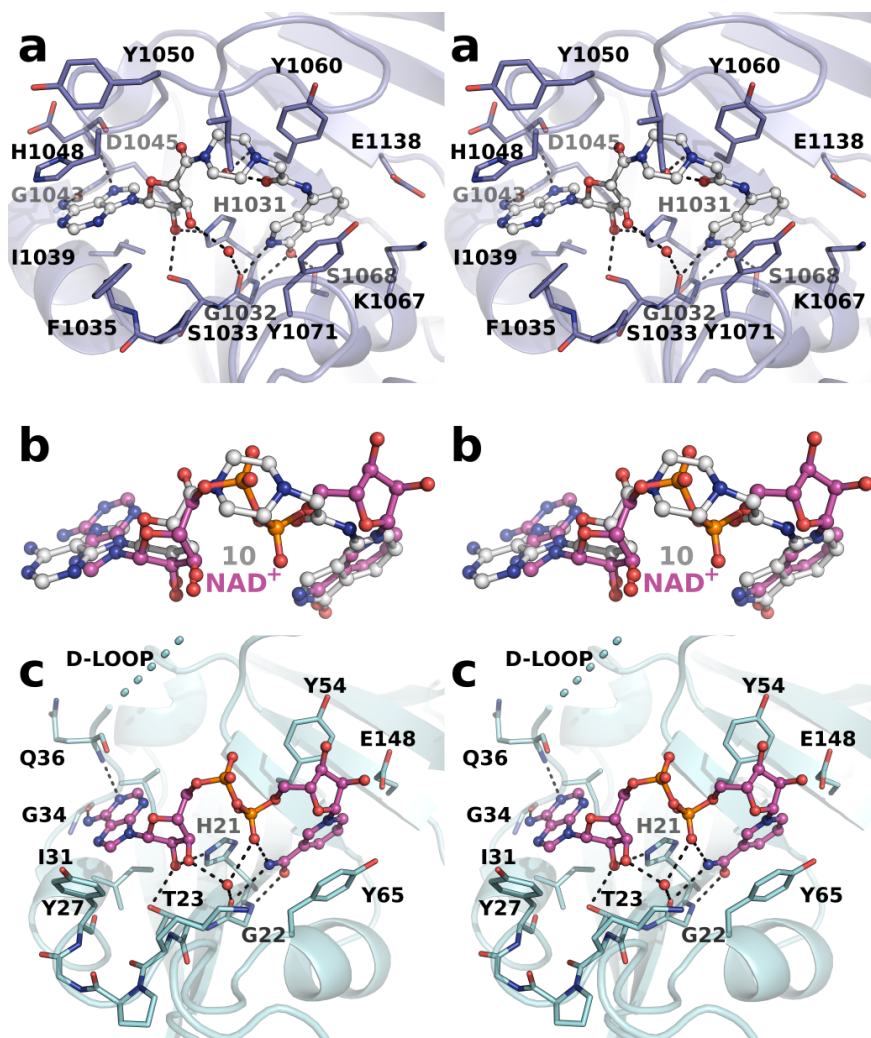
Figure 10. Stereo view of binding mode of compound 10 with TNKS2 and its comparison with NAD$^+$ bound diphtheria toxin crystal structure. (a) TNKS2 (blue colored) in complex with **10** (light grey); (b) comparison of superposed 10 with NAD$^+$ in diphtheria toxin; (c) NAD$^+$ bound diphtheria toxin (PDB code: 1TOX)

Notably, these amino acid residues are conserved in other members of ARTD enzyme superfamily. Furthermore, the adenosine moiety was situated between an α-helix and His1048 and it formed hydrogen bonds with the backbone atoms of Gly1043 and Asp1045 (**Fig. 10a**)

The comparison between **10** in complex with the TNKS2 catalytic domain and NAD$^+$ bound diphtheria toxin crystal structure (PDB code: 1TOX) (Bell & Eisenberg, 1997) showed that the overall binding mode of **10** is very similar to NAD$^+$ (**Fig. 10c**). Both NAD$^+$ and **10** did not make any interactions with the D-loop. In the co-crystal structure containing **10**, the adenosine moiety was rotated 180º in comparison to the ARTD1-NAD$^+$ complex structure (**Fig. 10c**).

In diphtheria toxin crystals, the adenosine region of the NAD$^+$ was hydrogen bonded to conserved amino acid residues His21 and Thr23, and also to a water molecule. Adenosine moiety also formed hydrogen bonds with Gly34 and Gln36 (**Fig. 10c**). The histidine, unique to tankyrases, that was stacking with **10** in the complex crystal structure, was also missing in the diphtheria toxin structure. These differences may therefore indicate that the binding mode in human ARTDs or in tankyrases could be distinct from the diphtheria toxin or the rotation could be just a property of the inhibitor.

5 Discussion

TNKS1 was first discovered 15 years ago and since then tankyrases have been implicated in many cellular processes (Smith *et al*, 1998). Their functions such as involvement in the telomere homeostasis and in the Wnt signaling have made them very interesting drug targets. Just after this PhD project was started, it was suggested that TNKS1 inhibition suppress the oncogenic Wnt signaling (Huang *et al*, 2009) and this directed many research groups to develop selective tankyrase inhibitors. At that moment, the field was very new and there was very little known about the possible small molecules that could inhibit tankyrases selectively. During this PhD project the field has grown tremendously and many research groups including ours have reported potent tankyrase inhibitors.

5.1 The screening assay (I, III, IV)

The first step towards the discovery of inhibitors was the development of an assay that could be used for screening the chemical libraries. There were some tankyrase assays available earlier, but it was difficult to evaluate the usefulness and robustness of those assays for screening. We adapted the assay developed for ARTD1 (Putt & Hergenrother, 2004) and optimized it for tankyrases. The assay was based on the automodification activity of enzymes, which means that tankyrases will act both as the enzyme and the target protein. The chemical reaction is based on the principle that *N*-alkylpyridinium compounds can be converted to fluorescent product through reaction with a ketone followed by heating in excess acid. All the chemical screening and potency measurements were performed at pH 7 because of its closeness to the physiological pH. Traditional PARP/ARTD phosphate buffer, pH 8, containing Mg^{2+} (Putt & Hergenrother, 2004) was not a good choice for TNKS1 activity. As TNKS1 was less active at pH 8 and Mg^{2+} was also inhibiting the enzyme activity. Different buffers and reagents were tested for enzyme activity and finally the most suitable of them was used depending upon the different constructs.

Assay performance was analyzed manually and with a pipetting robot. Signals were normally distributed and statistics showed that assay is robust for screening compounds. Incubation times were adjusted to achieve the high performance of the assay. It was observed that even with the manual setup, it was possible to screen hundreds or thousands of compounds per day. Assay was carried out using very low substrate concentration that made it sensitive to the competitive inhibitors.

There have been some ARTD assay reports earlier but they required special reagents such as colorimetric modification of the substrate NAD^+, bioNAD$^+$, or radiolabeled NAD^+ (Nottbohm *et al*, 2007; Schraufstatter *et al*, 1986; Zhang & Snyder, 1993). In comparison, the assay used here is very inexpensive and does not require any washing steps. In addition, it is possible to use the protein

purified using *E. coli* as host organism even with a single purification step without the need of any special kit. Previously, only two screening assays had been described for TNKS1. They were based on a colorimetric substrate variant and yeast cell-based screening method (Nottbohm *et al*, 2007; Yashiroda *et al*, 2010). In the colorimetric assay, the measurement could be done at any point, but the signal observed appears not to be as robust as with the fluorescence method. In the yeast based system, the yeast strains were used to overexpress TNKS1 and compounds were screened that can protect the cells against the TNKS1-induced growth arrest. Being a whole cell-based assay, there is possibility of detecting the nonspecific hits that can protect the cells by other mechanisms. In contrast to other assays, the biochemical assay used is high throughput, feasible, simple, has high DMSO tolerance, is compatible with the automatic system, and of low cost. This assay has also been successfully optimized for other ARTD members in our laboratory. Best buffers were selected depending on the enzymatic activity of ARTD members. In case of ARTD1 and ARTD2, activated DNA was added to the final buffer, whereas, an additional substrate protein was used with some mono ARTDs such as ARTD7 and ARTD10 (Haikarainen *et al*, 2013a, 2013b; Narwal *et al*, 2013b; Venkannagari *et al*, 2013).

A validatory screening was done in order to check the assay performance and results were confirmed with western blot. Hit limit was set to $2 \times SD$ to get more hit compounds in the initial stage of the screening and three of the hit compounds showed selectivity towards TNKS1 over ARTD1 and ARTD2. The potency value of flavone was measured with TNKS1 using the biochemical assay and the IC_{50}-value of 325 nM agreed well with the previous studies in yeast cell lysates (Yashiroda *et al*, 2010). In addition we measured potencies of the known potent tankyrase inhibitors XAV939 ($IC_{50} = 5$ nM) and IWR-1 ($IC_{50} = 64$ nM) against TNKS1, which were in accordance with the previously reported values (Huang *et al*, 2009).

5.2 Flavones as tankyrase inhibitors (III, IV)

Flavone has been identified as a TNKS1 inhibitor in a yeast-based screening method and also in our validatory screening using the natural compound library (Narwal *et al*, 2012a; Yashiroda *et al*, 2010). This raised the question, whether other classes of flavonoids would also be able to inhibit tankyrases. Flavonoids are secondary metabolites that are widely present in plant sources and in our daily diet (Aron & Kennedy, 2008; Benavente-García *et al*, 1997; Landete, 2012). They are further divided into various classes such as flavones, isoflavones, flavonones, anthocyanidines, flavanols, and flavonols (Harborne & Williams, 2000). It has been suggested that flavonoids have several beneficial properties such as antioxidant, neuroprotective, antiviral, and anticancer properties (Birt *et al*, 2001; Galati *et al*, 2000; Middleton *et al*, 2000; Yang *et al*, 2001). Flavonoids are also shown to have antiproliferative effects on several tumor cell lines (Kandaswami *et al*, 2005).

After discovering flavones as tankyrase inhibitors with selectivity over ARTD1, we decided to screen flavonoids against tankyrases (Narwal *et al*, 2013a) and a flavonoid library containing the 500 nature-inspired compounds was screened using TNKS2 catalytic domain. Screening results showed that flavones were the best inhibitors of TNKS2 among flavonoids and other classes did not inhibit TNKS2 at the tested concentration.

Flavones do not contain the characteristic nicotinamide motif. They lack the amide, which was thought to be required for efficient binding with the nicotinamide site of the enzyme. There was no crystal structure available before this project that could explain the binding of flavones. We solved the crystal structure of TNKS2 in complex with flavone (**Fig. 5a** in **III**) that showed that it binds to the same binding pocket as do most of the ARTD inhibitors. The interaction between the flavone carbon at position 3 and the carbonyl of the Gly1032 was the result of the partial charge distribution character of the hydrogen and C3 carbon (**Fig. 5a** in **III**). Most of the hit compounds identified in the flavonoids screening contained hydroxyl groups and they did not have a high impact on the potency of the compounds.

All the compounds showed similar potencies against both the tankyrases except for two compounds containing fluorine atom and methyl group substituted to position 4´ respectively, these compounds were actually selective towards TNKS1 over TNKS2. These differences could not be explained by the structural data as catalytic domains of both the tankyrases are almost identical. Our hypothesis was that, our TNKS1 fragment contains an additional SAM domain that could have improved the binding of compounds to TNKS1 by affecting the protein flexibility or by interacting with the binding cavity and enhancing the hydrophobic interactions between the compound and protein molecule. Later we were able to produce TNKS2 fragment containing the SAM and ARTD domains and we found that the presence of a SAM domain improved the potency of compounds by 2 to 3-fold. The SAM domain improves the enzyme activity so that protein was active even at very low nanomolar concentration. However, it does not completely explain the selectivity of inhibitors towards TNKS1 over TNKS2 or vice-versa.

Flavonoids have been shown to be associated with the antiproliferative effects (Asensi *et al*, 2011; Kandaswami *et al*, 2005) on the cancer cells, and some of their effects could be because of the tankyrase inhibition. Chemical space analysis of the flavonoid library showed that the flavones inhibiting tankyrases would be small and aromatic, and generally small substitutions would be tolerable (**Fig. 7** in **III**). Compounds that clustered around the hits were also flavones and were also inhibiting or close to the set hit limit in screening. The unfavorable binding of specific flavones is easily explainable with the crystal structure as there is no space to accommodate them in the binding cavity.

To get further insights about the flavones' selectivity towards tankyrases, we decided to screen the commercially available flavones containing single substitutions. A selection criterion was to discover compounds, which would be more potent in comparison to base compound flavone. Therefore, nineteen compounds were selected for the potency measurements on the basis of their inhibition at 1 µM. Co-crystal structures were also solved with all the hit compounds. It was observed that the position 4′ was best for substitutions (**Table 1** in **IV**), because it extends from the binding site towards the solvent. Position 6′ was also suitable for smaller substitutions but these did not improve the potency of the compounds. Substitution to 4′ position also led to more potent and selective inhibitors, as best compounds were containing hydrophobic substitutions to 4′ position. Compound **29** (**IV**) was the only compound that formed a direct hydrogen bond with the protein molecule. However, it did not show any inhibition in the cell based assay reporting the Wnt signaling inhibition. The potential reasons for the inactivity of the compounds could be nonspecific binding, cell permeability, compound solubility and stability. Therefore, *in vitro* biochemical assay and cell-based assay showed differences in the results.

The complex crystal structures showed that all the compounds bind to the nicotinamide site as expected. As nicotinamide site is conserved in the ARTD enzyme family, therefore, to confirm the selectivity, IC_{50}-values of the best compounds and XAV939 were measured with ARTD1, ARTD2, TNKS1 and TNKS2. Analysis of results showed that compound **22** (**Table 5b**) is more selective towards TNKS1 and also maintain similar potency as XAV939. Compound **22** (**Table 5b**) is most hydrophobic in the series with excellent ligand efficiency (Kuntz *et al*, 1999). **22** also maintains the lipophilic efficiency (Waring, 2010) at the same level as other potent compounds that were inhibiting Wnt signaling.

In general, the IC_{50}-values of the compounds were better for TNKS1 over TNKS2. We were expecting that larger substitutions to position 4′ might be better for selectivity as compounds extending in this direction would clash with the AH regulatory domain present in ARTD1-ARTD4, but not in ARTD5-ARTD17 (Karlberg *et al*, 2010; Narwal *et al*, 2013a). However, this was not the case as the largest compound, **27** (**Table 5b**), showed inhibition of ARTD1 at 1 µM concentration (**Fig. 2** in **IV**). Our view is that some of the compounds possibly interacted with the highly polar binding site of ARTD1-4 (Wahlberg *et al*, 2012), and also had interaction with the AH regulatory domain present in these enzymes.

Our results showed that it is possible to create selective tankyrase inhibitors binding to nicotinamide site. The molecular details shown by the co-crystal structures could be utilized in predicting and further optimizing the flavones and related compounds for higher potency.

5.3   Novel binding mode of IWR-1 (II)

IWR-1 (**Fig. 6**) was identified in the STF assay as a tankyrase inhibitor. We solved the crystal structure of the TNKS2 in complex with IWR-1. Complex crystal structure showed that IWR-1 was the first compound binding to the adenosine site rather than to nicotinamide site (**Fig. 3c** in **II**). IWR-1 binding induced changes in the protein molecule at the nicotinamide-binding site, but most importantly it caused the opening of the D-loop. Structure-activity relationship analysis showed that these changes were required for the high potency of the compound. All three regions of the compound; amide, spacer and norbornyl were required and modifications of them led to lower potency or completely abolished the activity in Wnt signaling assay. The superposition of TNKS2-IWR-1 complex structure with ARTD1 showed that some of the interactions made by norbornyl region of the compound are conserved or complementary to TNKS2. However, clashes were observed between AH protein regulatory domain of ARTD1 and compound. This indicated that ARTD1 domains need to open to accommodate IWR-1. The absence of required interactions and movement of domains in ARTD1 are major reasons behind the selectivity of IWR-1 towards tankrases.

This complex crystal structure showed that targeting the adenosine site could lead to selective inhibition of tankyrases. The unique interaction between the compound and protein molecule has defined a new pharmacophore model and has already been used in the design of new inhibitors (Bregman *et al*, 2013a).

5.4   Inhibition of tankyrases by ARTD inhibitors (V)

A small library of ARTD inhibitors and analogues was screened against TNKS1. Their binding modes were studied using protein X-ray crystallography. In order to identify the potent tankyrase inhibitors, compounds were screened at final concentration of 500 nM. Nine compounds showed more than 20 % inhibition at this concentration, therefore, these compounds were selected further for characterization using a biochemical assay and crystallography. Co-crystal structures of TNKS2 in complex with potent tricyclic compounds phenanthridinone and TIQ-A (**Fig. 9**) showed that the inhibitors were compatible with the closed conformation of the D-loop and formed the hydrophobic interactions with the neighboring residues. These interactions are conserved in tankyrases and these compounds were slightly selective towards tankyrases over ARTD1. Screening results showed that, the clinical candidates against ARTD1, veliparib and iniparib displayed only 33 % inhibition and no inhibition of TNKS1 at 10 μM, respectively. Binding of PJ-34 (**17**) and rucaparib (**29**) caused disordering of the D-loop. Consequently, PJ-34 displayed lower potencies (TNKS1 1300 nM; TNKS2 219 nM), whereas, rucaparib showed low IC$_{50}$-values (TNKS1 25 nM; TNKS2 14 nM) (**Fig. 9**). Therefore, some of the effects of

rucaparib shown in the earlier studies as ARTD1 inhibitor could also be affected by tankyrase inhibition.

5.5 Substrate binding (II, V)

To date, there is no structural information available that could shed light on the molecular interactions between NAD^+ and any human ARTD member. Therefore, in order to get further insights, we tried to soak the TNKS2 crystal with the solution containing high concentrations of NAD^+, but soaking resulted in the binding of only a byproduct nicotinamide. This indicated that chymotrypsin cleaved enzyme used in the crystallization could hydrolyze NAD^+. The western blot results showed that it could also catalyze covalent automodification reaction. However enzymatic activity was lower for the cleaved enzyme. Nicotinamide made the conserved interactions with the TNKS2 ARTD domain. The crystal structure showed that TNKS2 catalytic domain could accommodate inhibitors without disturbing the crystal packing and could be utilized in finding new inhibitors.

EB-47 (Compound **10**) (**Fig. 9**), NAD^+ mimic compound, was soaked with TNKS2 crystals to evaluate ARTD inhibitors against tankyrases, and some indications of NAD^+ binding can be deduced from the solved crystal structure. Superposing the NAD^+ bound diphtheria toxin crystal structure (PDB code: 1TOX) with TNKS2-**10** complex structure showed that overall the conformation was very similar but there were differences especially at the adenosine moiety, which has been rotated by 180 degrees in the EB-47. Interestingly, neither NAD^+ (PDB code: 1TOX) nor EB-47 made any specific interactions with the D-loop and region was not resolved in the electron density in the NAD^+ bound diphtheria toxin crystal structure. The substrate could have any of the mentioned interactions made by EB-47 with TNKS2 or NAD^+ in diphtheria toxin.

Compound **10** is not the actual substrate and has differences in the chemical structure compared to NAD^+, as it does not contain the diphosphate and ribose parts of substrate. This could cause changes also in the binding of nicotinamide and adenosine mimicking moieties. However, from the comparison of complex crystal structures of TNKS2-**10** and previously reported diphtheria toxin-NAD^+, it is evident that catalytic glutamate of TNKS2 would be close enough (~ 2.9 Å) to NAD^+ ribose, missing in compound **10**. It would stabilize the the oxacarbenium ion transition state through electrostatic interaction, required for catalysis of NAD^+ (Kleine *et al*, 2008). The crystal structures in complex with nicotinamide and EB-47, as well as comparisons with diphtheria toxin structure forms our current view of the substrate and byproduct binding to tankyrases. The mechanism of ADP-ribose transfer in tankyrases and other ARTDs requires more research and structures in complex with NAD^+ and an acceptor molecule would give an insight on the molecular details of the reaction.

6 Conclusions and future perspectives

Tankyrases are implicated in many cellular processes and are emerging as potential drug targets. Therefore, there has been growing interest towards discovering and designing new inhibitors against them. This thesis work was also focused on discovering selective and potent tankyrase inhibitors, as there were no specific tankyrase inhibitors available before this project was started.

Important conclusions drawn from this study are:

1. Fluorescence-based activity assay developed during this study is suitable for screening the chemical libraries and to measure the IC_{50}-values. Good Z´-value, simplicity, feasibility, low cost, high DMSO tolerance also made this homogeneous activity assay suitable for high throughput screening of compounds. Activity assay described for TNKS1 is optimized for TNKS2 catalytic domain and calculations of assay parameters confirmed its suitability for screening.

2. Flavones bind to nicotinamide binding site in the NAD^+ binding groove. However, they are missing the amide present in other inhibitors binding to nicotinamide binding site. They are the most potent inhibitors of tankyrases among different classes of flavonoids.

3. It is possible to create potent tankyrase inhibitors utilizing the flavone scaffold. Para position of the phenyl ring is best to introduce substitutions in order to increase the potency. Substitutions at other sites do not increase the potency or cause loss of activity. Hydrophobic substitutions at 4´-position increase the selectivity toward tankyrases. Despite the conserved binding site, hit compounds showed nanomolar potency and isoenzyme selectivity for tankyrases and efficiently inhibited the Wnt signaling in a cell-based assay.

4. IWR-1 was the first compound that was shown to bind to adenosine site in the binding motif. Co-crystal structure of TNKS2 with IWR-1 showed that compound utilized the flexibility of the D-loop to bind to the NAD^+ binding groove.

5. Co-crystal structure of TNKS 2 with EB-47 (NAD^+ mimic compound) allowed to analyze the substrate binding mode. Soaking NAD^+ to TNKS2 crystals led to nicotinamide-bound complex that showed the interactions made by nicotinamide with protein molecule.

6. Evaluation of known small molecule inhibitors of ARTD1 against tankyrases showed that some of the compounds are also potent tankyrase inhibitors. This could affect the studies done with these compounds including the outcomes of clinical trials with ARTD1 inhibitors.

In general, inhibitor discovery in the ARTD field has mostly been focused on nicotinamide site. However, after TNKS2-IWR-1 complex structure, IWR-1 scaffold has also been optimized and potency has been improved from 130 nM to

1 nM using molecular modeling and structure-based drug design (Bregman *et al*, 2013a). The potency measurements and analysis of crystal structures have shown that tankyrase inhibitors binding to adenosine site are in general more selective towards tankyrases in comparison to compounds binding to the nicotinamide site (Haikarainen *et al*, 2013b; Shultz *et al*, 2012; Voronkov *et al*, 2013). There have also been efforts to develop dual binders that bind to both sites of the NAD^+ binding cleft (Bregman *et al*, 2013b; Shultz *et al*, 2013a).

Recently, it was shown that colorectal tumor growth developed by the mutation in *APC* gene could be suppressed by small-molecule tankyrase inhibitors G007-LK and G244-LM (Lau *et al*, 2013). Tankyrase inhibition led to the inhibition of Wnt signaling and consequently destabilization of β-catenin. However, this also affected cell proliferation and caused toxicity in the intestinal gland, a probable on-target effect, which has raised questions on utilization of tankyrase inhibitors in cancer therapy. In future, these questions should be addressed and research should be done to clearly define the role of tankyrase in cancer or other diseases.

In summary, inhibitors binding to the nicotinamide site were discovered and selective nature of an adenosine site binding inhibitor was studied. The biochemical assay will be useful for *in vitro* screening of compounds and extensive crystallographic work conducted in this thesis will hopefully facilitate further development of tankyrase inhibitors.

7 References

Altmeyer M, Messner S, Hassa PO, Fey M & Hottiger MO (2009a) Molecular mechanism of poly(ADP-ribosyl)ation by PARP1 and identification of lysine residues as ADP-ribose acceptor sites. *Nucleic Acids Res.* **37:** 3723–3738

Altmeyer M, Messner S, Hassa PO, Fey M & Hottiger MO (2009b) Molecular mechanism of poly(ADP-ribosyl)ation by PARP1 and identification of lysine residues as ADP-ribose acceptor sites. *Nucleic Acids Res.* **37:** 3723–3738

Alvarez-Gonzalez R & Jacobson MK (1987) Characterization of polymers of adenosine diphosphate ribose generated in vitro and in vivo. *Biochemistry (Mosc.)* **26:** 3218–3224

Amé JC, Rolli V, Schreiber V, Niedergang C, Apiou F, Decker P, Muller S, Höger T, Ménissier-de Murcia J & de Murcia G (1999) PARP-2, A novel mammalian DNA damage-dependent poly(ADP-ribose) polymerase. *J. Biol. Chem.* **274:** 17860–17868

Aron PM & Kennedy JA (2008) Flavan-3-ols: nature, occurrence and biological activity. *Mol. Nutr. Food Res.* **52:** 79–104

Asensi M, Ortega A, Mena S, Feddi F & Estrela JM (2011) Natural polyphenols in cancer therapy. *Crit. Rev. Clin. Lab. Sci.* **48:** 197–216

Augustin A, Spenlehauer C, Dumond H, Ménissier-De Murcia J, Piel M, Schmit A-C, Apiou F, Vonesch J-L, Kock M, Bornens M & De Murcia G (2003) PARP-3 localizes preferentially to the daughter centriole and interferes with the G1/S cell cycle progression. *J. Cell Sci.* **116:** 1551–1562

Bader M, Benjamin S, Wapinski OL, Smith DM, Goldberg AL & Steller H (2011) A conserved F box regulatory complex controls proteasome activity in Drosophila. *Cell* **145:** 371–382

Bae J, Donigian JR & Hsueh AJW (2003) Tankyrase 1 interacts with Mcl-1 proteins and inhibits their regulation of apoptosis. *J. Biol. Chem.* **278:** 5195–5204

Banasik M, Komura H, Shimoyama M & Ueda K (1992) Specific inhibitors of poly(ADP-ribose) synthetase and mono(ADP-ribosyl)transferase. *J. Biol. Chem.* **267:** 1569–1575

Barth E, Radermacher P & Szabó C (2006) The world according to poly(ADP-ribose) polymerase (PARP)--update 2006. *Intensive Care Med.* **32:** 1470–1474

Belenky P, Bogan KL & Brenner C (2007) NAD+ metabolism in health and disease. *Trends Biochem. Sci.* **32:** 12–19

Bell CE & Eisenberg D (1997) Crystal structure of diphtheria toxin bound to nicotinamide adenine dinucleotide. *Adv. Exp. Med. Biol.* **419:** 35–43

Benavente-García O, Castillo J, Marin FR, Ortuño A & Del Río JA (1997) Uses and Properties of Citrus Flavonoids. *J. Agric. Food Chem.* **45:** 4505–4515

Birt DF, Hendrich S & Wang W (2001) Dietary agents in cancer prevention: flavonoids and isoflavonoids. *Pharmacol. Ther.* **90:** 157–177

Bisht KK, Dudognon C, Chang WG, Sokol ES, Ramirez A & Smith S (2012) GDP-mannose-4,6-dehydratase is a cytosolic partner of tankyrase 1 that inhibits its poly(ADP-ribose) polymerase activity. *Mol. Cell. Biol.* **32:** 3044–3053

Boehler C, Gauthier LR, Mortusewicz O, Biard DS, Saliou J-M, Bresson A, Sanglier-Cianferani S, Smith S, Schreiber V, Boussin F & Dantzer F (2011) Poly(ADP-ribose) polymerase 3 (PARP3), a newcomer in cellular response to DNA damage and mitotic progression. *Proc. Natl. Acad. Sci. U. S. A.* **108:** 2783–2788

Bollini S, Herbst JJ, Gaughan GT, Verdoorn TA, Ditta J, Dubowchik GM & Vinitsky A (2002) High-throughput fluorescence polarization method for identification of FKBP12 ligands. *J. Biomol. Screen. Off. J. Soc. Biomol. Screen.* **7:** 526–530

Bork P, Hofmann K, Bucher P, Neuwald AF, Altschul SF & Koonin EV (1997) A

superfamily of conserved domains in DNA damage-responsive cell cycle checkpoint proteins. *FASEB J. Off. Publ. Fed. Am. Soc. Exp. Biol.* **11:** 68–76

Bregman H, Chakka N, Guzman-Perez A, Gunaydin H, Gu Y, Huang X, Berry V, Liu J, Teffera Y, Huang L, Egge B, Mullady EL, Schneider S, Andrews PS, Mishra A, Newcomb J, Serafino R, Strathdee CA, Turci SM, Wilson C, et al (2013a) Discovery of novel, induced-pocket binding oxazolidinones as potent, selective, and orally bioavailable tankyrase inhibitors. *J. Med. Chem.* **56:** 4320–4342

Bregman H, Gunaydin H, Gu Y, Schneider S, Wilson C, DiMauro EF & Huang X (2013b) Discovery of a class of novel tankyrase inhibitors that bind to both the nicotinamide pocket and the induced pocket. *J. Med. Chem.* **56:** 1341–1345

Busch AM, Johnson KC, Stan RV, Sanglikar A, Ahmed Y, Dmitrovsky E & Freemantle SJ (2013) Evidence for tankyrases as antineoplastic targets in lung cancer. *BMC Cancer* **13:** 211

Callow MG, Tran H, Phu L, Lau T, Lee J, Sandoval WN, Liu PS, Bheddah S, Tao J, Lill JR, Hongo J-A, Davis D, Kirkpatrick DS, Polakis P & Costa M (2011) Ubiquitin ligase RNF146 regulates tankyrase and Axin to promote Wnt signaling. *PloS One* **6:** e22595

Casás-Selves M, Kim J, Zhang Z, Helfrich BA, Gao D, Porter CC, Scarborough HA, Bunn PA Jr, Chan DC, Tan AC & DeGregori J (2012) Tankyrase and the canonical Wnt pathway protect lung cancer cells from EGFR inhibition. *Cancer Res.* **72:** 4154–4164

Chambon P, WEILL JD & MANDEL P (1963) Nicotinamide mononucleotide activation of new DNA-dependent polyadenylic acid synthesizing nuclear enzyme. *Biochem. Biophys. Res. Commun.* **11:** 39–43

Chang P, Coughlin M & Mitchison TJ (2005a) Tankyrase-1 polymerization of poly(ADP-ribose) is required for spindle structure and function. *Nat. Cell Biol.* **7:** 1133–1139

Chang W, Dynek JN & Smith S (2005b) NuMA is a major acceptor of poly(ADP-ribosyl)ation

by tankyrase 1 in mitosis. *Biochem. J.* **391:** 177–184

Chi NW & Lodish HF (2000) Tankyrase is a golgi-associated mitogen-activated protein kinase substrate that interacts with IRAP in GLUT4 vesicles. *J. Biol. Chem.* **275:** 38437–38444

Chiang YJ, Hsiao SJ, Yver D, Cushman SW, Tessarollo L, Smith S & Hodes RJ (2008) Tankyrase 1 and Tankyrase 2 Are Essential but Redundant for Mouse Embryonic Development. *PLoS ONE* **3:** e2639

Chiarugi A, Meli E, Calvani M, Picca R, Baronti R, Camaioni E, Costantino G, Marinozzi M, Pellegrini-Giampietro DE, Pellicciari R & Moroni F (2003) Novel isoquinolinone-derived inhibitors of poly(ADP-ribose) polymerase-1: pharmacological characterization and neuroprotective effects in an in vitro model of cerebral ischemia. *J. Pharmacol. Exp. Ther.* **305:** 943–949

Cho-Park PF & Steller H (2013) Proteasome Regulation by ADP-Ribosylation. *Cell* **153:** 614–627

Chu-Ping M, Slaughter CA & DeMartino GN (1992) Purification and characterization of a protein inhibitor of the 20S proteasome (macropain). *Biochim. Biophys. Acta* **1119:** 303–311

Clark JB, Ferris GM & Pinder S (1971) Inhibition of nuclear NAD nucleosidase and poly ADP-ribose polymerase activity from rat liver by nicotinamide and 5'-methyl nicotinamide. *Biochim. Biophys. Acta* **238:** 82–85

Cockman ME, Webb JD, Kramer HB, Kessler BM & Ratcliffe PJ (2009) Proteomics-based identification of novel factor inhibiting hypoxia-inducible factor (FIH) substrates indicates widespread asparaginyl hydroxylation of ankyrin repeat domain-containing proteins. *Mol. Cell. Proteomics MCP* **8:** 535–546

Cook BD, Dynek JN, Chang W, Shostak G & Smith S (2002) Role for the related poly(ADP-Ribose) polymerases tankyrase 1 and 2 at human telomeres. *Mol. Cell. Biol.* **22:** 332–342

Counter CM, Botelho FM, Wang P, Harley CB & Bacchetti S (1994) Stabilization of short

telomeres and telomerase activity accompany immortalization of Epstein-Barr virus-transformed human B lymphocytes. *J. Virol.* **68:** 3410–3414

D'Silva I, Pelletier JD, Lagueux J, D'Amours D, Chaudhry MA, Weinfeld M, Lees-Miller SP & Poirier GG (1999) Relative affinities of poly(ADP-ribose) polymerase and DNA-dependent protein kinase for DNA strand interruptions. *Biochim. Biophys. Acta* **1430:** 119–126

Deng Z, Atanasiu C, Zhao K, Marmorstein R, Sbodio JI, Chi N-W & Lieberman PM (2005) Inhibition of Epstein-Barr virus OriP function by tankyrase, a telomere-associated poly-ADP ribose polymerase that binds and modifies EBNA1. *J. Virol.* **79:** 4640–4650

Deng Z, Lezina L, Chen C-J, Shtivelband S, So W & Lieberman PM (2002) Telomeric proteins regulate episomal maintenance of Epstein-Barr virus origin of plasmid replication. *Mol. Cell* **9:** 493–503

Distler A, Deloch L, Huang J, Dees C, Lin N-Y, Palumbo-Zerr K, Beyer C, Weidemann A, Distler O, Schett G & Distler JHW (2012) Inactivation of tankyrases reduces experimental fibrosis by inhibiting canonical Wnt signalling. *Ann. Rheum. Dis.* **72:** 1575–1580

Dodson EJ, Winn M & Ralph A (1997) Collaborative Computational Project, number 4: providing programs for protein crystallography. *Methods Enzymol.* **277:** 620–633

Donigian JR & de Lange T (2007) The role of the poly(ADP-ribose) polymerase tankyrase1 in telomere length control by the TRF1 component of the shelterin complex. *J. Biol. Chem.* **282:** 22662–22667

Druzhyna N, Smulson ME, LeDoux SP & Wilson GL (2000) Poly(ADP-ribose) polymerase facilitates the repair of N-methylpurines in mitochondrial DNA. *Diabetes* **49:** 1849–1855

Dunstan MS, Barkauskaite E, Lafite P, Knezevic CE, Brassington A, Ahel M, Hergenrother PJ, Leys D & Ahel I (2012) Structure and mechanism of a canonical poly(ADP-ribose) glycohydrolase. *Nat. Commun.* **3:** 878

Dynek JN & Smith S (2004) Resolution of sister telomere association is required for progression through mitosis. *Science* **304:** 97–100

Emsley P & Cowtan K (2004) Coot: model-building tools for molecular graphics. *Acta Crystallogr. D Biol. Crystallogr.* **60:** 2126–2132

Feijs KLH, Verheugd P & Lüscher B (2013) Expanding functions of intracellular resident mono-ADP-ribosylation in cell physiology. *FEBS J.* **280:** 3519–3529

Fuchs U, Rehkamp GF, Slany R, Follo M & Borkhardt A (2003) The formin-binding protein 17, FBP17, binds via a TNKS binding motif to tankyrase, a protein involved in telomere maintenance. *FEBS Lett.* **554:** 10–16

Gagné J-P, Hendzel MJ, Droit A & Poirier GG (2006) The expanding role of poly(ADP-ribose) metabolism: current challenges and new perspectives. *Curr. Opin. Cell Biol.* **18:** 145–151

Galati G, Teng S, Moridani MY, Chan TS & O'Brien PJ (2000) Cancer chemoprevention and apoptosis mechanisms induced by dietary polyphenolics. *Drug Metabol. Drug Interact.* **17:** 311–349

Gao J, Zhang J, Long Y, Tian Y & Lu X (2011) Expression of tankyrase 1 in gastric cancer and its correlation with telomerase activity. *Pathol. Oncol. Res. POR* **17:** 685–690

Gelmini S, Poggesi M, Distante V, Bianchi S, Simi L, Luconi M, Raggi CC, Cataliotti L, Pazzagli M & Orlando C (2004) Tankyrase, a positive regulator of telomere elongation, is over expressed in human breast cancer. *Cancer Lett.* **216:** 81–87

Gelmini S, Poggesi M, Pinzani P, Mannurita SC, Cianchi F, Valanzano R & Orlando C (2006) Distribution of Tankyrase-1 mRNA expression in colon cancer and its prospective correlation with progression stage. *Oncol. Rep.* **16:** 1261–1266

Glickman MH & Ciechanover A (2002) The ubiquitin-proteasome proteolytic pathway: destruction for the sake of construction. *Physiol. Rev.* **82:** 373–428

Goldberg AL (2007) On prions, proteasomes, and mad cows. *N. Engl. J. Med.* **357:** 1150–1152

Gonzalez-Rey E, Martínez-Romero R, O'Valle F, Aguilar-Quesada R, Conde C, Delgado M & Oliver FJ (2007) Therapeutic effect of a poly(ADP-ribose) polymerase-1 inhibitor on experimental arthritis by downregulating inflammation and Th1 response. *PloS One* **2:** e1071

Guettler S, LaRose J, Petsalaki E, Gish G, Scotter A, Pawson T, Rottapel R & Sicheri F (2011) Structural basis and sequence rules for substrate recognition by Tankyrase explain the basis for cherubism disease. *Cell* **147:** 1340–1354

Guo H-L, Zhang C, Liu Q, Li Q, Lian G, Wu D, Li X, Zhang W, Shen Y, Ye Z, Lin S-Y & Lin S-C (2012) The Axin/TNKS complex interacts with KIF3A and is required for insulin-stimulated GLUT4 translocation. *Cell Res.* **22:** 1246–1257

Ha G-H, Kim H-S, Go H, Lee H, Seimiya H, Chung DH & Lee C-W (2012) Tankyrase-1 function at telomeres and during mitosis is regulated by Polo-like kinase-1-mediated phosphorylation. *Cell Death Differ.* **19:** 321–332

Haikarainen T, Koivunen J, Narwal M, Venkannagari H, Obaji E, Joensuu P, Pihlajaniemi T & Lehtiö L (2013a) para-Substituted 2-Phenyl-3,4-dihydroquinazolin-4-ones As Potent and Selective Tankyrase Inhibitors. *ChemMedChem* **8:** 1978–1985

Haikarainen T, Venkannagari H, Narwal M, Obaji E, Lee H-W, Nkizinkiko Y & Lehtiö L (2013b) Structural Basis and Selectivity of Tankyrase Inhibition by a Wnt Signaling Inhibitor WIKI4. *PloS One* **8:** e65404

Harborne JB & Williams CA (2000) Advances in flavonoid research since 1992. *Phytochemistry* **55:** 481–504

Hart M, Concordet JP, Lassot I, Albert I, del los Santos R, Durand H, Perret C, Rubinfeld B, Margottin F, Benarous R & Polakis P (1999) The F-box protein beta-TrCP associates with phosphorylated beta-catenin and regulates its activity in the cell. *Curr. Biol. CB* **9:** 207–210

Hassa PO & Hottiger MO (2008) The diverse biological roles of mammalian PARPS, a small but powerful family of poly-ADP-ribose polymerases. *Front. Biosci. J. Virtual Libr.* **13:** 3046–3082

Her YR & Chung IK (2009) Ubiquitin Ligase RLIM Modulates Telomere Length Homeostasis through a Proteolysis of TRF1. *J. Biol. Chem.* **284:** 8557–8566

Hershko A & Ciechanover A (1998) The ubiquitin system. *Annu. Rev. Biochem.* **67:** 425–479

Hilton JF, Hadfield MJ, Tran M-T & Shapiro GI (2013) Poly(ADP-ribose) polymerase inhibitors as cancer therapy. *Front. Biosci. Landmark Ed.* **18:** 1392–1406

Hinney A & Hebebrand J (2009) Three at one swoop! *Obes. Facts* **2:** 3–8

Hofker M & Wijmenga C (2009) A supersized list of obesity genes. *Nat. Genet.* **41:** 139–140

Hottiger MO, Hassa PO, Lüscher B, Schüler H & Koch-Nolte F (2010) Toward a unified nomenclature for mammalian ADP-ribosyltransferases. *Trends Biochem. Sci.* **35:** 208–219

Hou JC & Pessin JE (2007) Ins (endocytosis) and outs (exocytosis) of GLUT4 trafficking. *Curr. Opin. Cell Biol.* **19:** 466–473

Hsiao SJ & Smith S (2008) Tankyrase function at telomeres, spindle poles, and beyond. *Biochimie* **90:** 83–92

Huang M, Wang Y, Sun D, Zhu H, Yin Y, Zhang W, Yang S, Quan L, Bai J, Wang S, Chen Q, Li S & Xu N (2006) Identification of genes regulated by Wnt/beta-catenin pathway and involved in apoptosis via microarray analysis. *BMC Cancer* **6:** 221

Huang S-MA, Mishina YM, Liu S, Cheung A, Stegmeier F, Michaud GA, Charlat O, Wiellette E, Zhang Y, Wiessner S, Hild M, Shi X, Wilson CJ, Mickanin C, Myer V, Fazal A, Tomlinson R, Serluca F, Shao W, Cheng H, et al (2009) Tankyrase inhibition stabilizes axin and antagonizes Wnt signalling. *Nature* **461:** 614–620

Iversen PW, Eastwood BJ, Sittampalam GS & Cox KL (2006) A comparison of assay performance measures in screening assays: signal window, Z' factor, and assay variability ratio. *J. Biomol. Screen.* **11:** 247–252

Jagtap PG, Southan GJ, Baloglu E, Ram S, Mabley JG, Marton A, Salzman A & Szabó C (2004) The discovery and synthesis of novel adenosine substituted 2,3-dihydro-1H-isoindol-1-ones: potent inhibitors of poly(ADP-ribose) polymerase-1 (PARP-1). *Bioorg. Med. Chem. Lett.* **14:** 81–85

James RG, Davidson KC, Bosch KA, Biechele TL, Robin NC, Taylor RJ, Major MB, Camp ND, Fowler K, Martins TJ & Moon RT (2012) WIKI4, a novel inhibitor of tankyrase and Wnt/ß-catenin signaling. *PloS One* **7:** e50457

Juarez-Salinas H, Levi V, Jacobson EL & Jacobson MK (1982) Poly(ADP-ribose) has a branched structure in vivo. *J. Biol. Chem.* **257:** 607–609

Juarez-Salinas H, Mendoza-Alvarez H, Levi V, Jacobson MK & Jacobson EL (1983) Simultaneous determination of linear and branched residues in poly(ADP-ribose). *Anal. Biochem.* **131:** 410–418

Kabsch W (2010) XDS. *Acta Crystallogr. D Biol. Crystallogr.* **66:** 125–132

Kanai M, Miwa M, Kuchino Y & Sugimura T (1982) Presence of branched portion in poly(adenosine diphosphate ribose) in vivo. *J. Biol. Chem.* **257:** 6217–6223

Kandaswami C, Kanadaswami C, Lee L-T, Lee P-PH, Hwang J-J, Ke F-C, Huang Y-T & Lee M-T (2005) The antitumor activities of flavonoids. *Vivo Athens Greece* **19:** 895–909

Karlberg T, Markova N, Johansson I, Hammarström M, Schütz P, Weigelt J & Schüler H (2010) Structural basis for the interaction between tankyrase-2 and a potent Wnt-signaling inhibitor. *J. Med. Chem.* **53:** 5352–5355

Kickhoefer VA, Siva AC, Kedersha NL, Inman EM, Ruland C, Streuli M & Rome LH (1999) The 193-kD vault protein, VPARP, is a novel poly(ADP-ribose) polymerase. *J. Cell Biol.* **146:** 917–928

Kim MK, Dudognon C & Smith S (2012) Tankyrase 1 regulates centrosome function by controlling CPAP stability. *EMBO Rep.* **13:** 724–732

Kim MS, An CH, Kim SS, Yoo NJ & Lee SH (2011) Frameshift mutations of poly(adenosine diphosphate-ribose) polymerase genes in gastric and colorectal cancers with microsatellite instability. *Hum. Pathol.* **42:** 1289–1296

Kirby CA, Cheung A, Fazal A, Shultz MD & Stams T (2012) Structure of human tankyrase 1 in complex with small-molecule inhibitors PJ34 and XAV939. *Acta Crystallograph. Sect. F Struct. Biol. Cryst. Commun.* **68:** 115–118

Kleine H, Poreba E, Lesniewicz K, Hassa PO, Hottiger MO, Litchfield DW, Shilton BH & Lüscher B (2008) Substrate-assisted catalysis by PARP10 limits its activity to mono-ADP-ribosylation. *Mol. Cell* **32:** 57–69

Koch-Nolte F, Haag F, Guse AH, Lund F & Ziegler M (2009) Emerging roles of NAD+ and its metabolites in cell signaling. *Sci. Signal.* **2:** mr1

Koch-Nolte F, Kernstock S, Mueller-Dieckmann C, Weiss MS & Haag F (2008) Mammalian ADP-ribosyltransferases and ADP-ribosylhydrolases. *Front. Biosci. J. Virtual Libr.* **13:** 6716–6729

Koh DW, Dawson TM & Dawson VL (2005) Mediation of cell death by poly(ADP-ribose) polymerase-1. *Pharmacol. Res. Off. J. Ital. Pharmacol. Soc.* **52:** 5–14

Kuntz ID, Chen K, Sharp KA & Kollman PA (1999) The maximal affinity of ligands. *Proc. Natl. Acad. Sci. U. S. A.* **96:** 9997–10002

Kutuzov MM, Khodyreva SN, Amé J-C, Ilina ES, Sukhanova MV, Schreiber V & Lavrik OI (2013) Interaction of PARP-2 with DNA structures mimicking DNA repair intermediates and consequences on activity of base excision repair proteins. *Biochimie* **95:** 1208–1215

Landete JM (2012) Updated knowledge about polyphenols: functions, bioavailability, metabolism, and health. *Crit. Rev. Food Sci. Nutr.* **52:** 936–948

Langelier M-F, Planck JL, Roy S & Pascal JM (2011) Crystal structures of poly(ADP-ribose) polymerase-1 (PARP-1) zinc fingers bound to DNA: structural and functional insights into DNA-dependent PARP-1 activity. *J. Biol. Chem.* **286:** 10690–10701

Langelier M-F, Planck JL, Roy S & Pascal JM (2012) Structural basis for DNA damage-dependent poly(ADP-ribosyl)ation by human PARP-1. *Science* **336:** 728–732

Langelier M-F, Ruhl DD, Planck JL, Kraus WL & Pascal JM (2010) The Zn3 domain of human poly(ADP-ribose) polymerase-1 (PARP-1) functions in both DNA-dependent poly(ADP-ribose) synthesis activity and chromatin compaction. *J. Biol. Chem.* **285:** 18877–18887

Langelier M-F, Servent KM, Rogers EE & Pascal JM (2008) A third zinc-binding domain of human poly(ADP-ribose) polymerase-1 coordinates DNA-dependent enzyme activation. *J. Biol. Chem.* **283:** 4105–4114

Lau T, Chan E, Callow M, Waaler J, Boggs J, Blake RA, Magnuson S, Sambrone A, Schutten M, Firestein R, Machon O, Korinek V, Choo E, Diaz D, Merchant M, Polakis P, Holsworth DD, Krauss S & Costa M (2013) A novel tankyrase small-molecule inhibitor suppresses APC mutation-driven colorectal tumor growth. *Cancer Res.* **73:** 3132–3144

Laurençot CM, Scheffer GL, Scheper RJ & Shoemaker RH (1997) Increased LRP mRNA expression is associated with the MDR phenotype in intrinsically resistant human cancer cell lines. *Int. J. Cancer J. Int. Cancer* **72:** 1021–1026

Lee TH, Perrem K, Harper JW, Lu KP & Zhou XZ (2006) The F-box protein FBX4 targets PIN2/TRF1 for ubiquitin-mediated degradation and regulates telomere maintenance. *J. Biol. Chem.* **281:** 759–768

Lehtiö L, Collins R, van den Berg S, Johansson A, Dahlgren L-G, Hammarström M, Helleday T, Holmberg-Schiavone L, Karlberg T & Weigelt J (2008) Zinc binding catalytic domain of human tankyrase 1. *J. Mol. Biol.* **379:** 136–145

Leney SE & Tavaré JM (2009) The molecular basis of insulin-stimulated glucose uptake: signalling, trafficking and potential drug targets. *J. Endocrinol.* **203:** 1–18

Levaot N, Voytyuk O, Dimitriou I, Sircoulomb F, Chandrakumar A, Deckert M, Krzyzanowski PM, Scotter A, Gu S, Janmohamed S, Cong F, Simoncic PD, Ueki Y, La Rose J & Rottapel

R (2011) Loss of Tankyrase-mediated destruction of 3BP2 is the underlying pathogenic mechanism of cherubism. *Cell* **147:** 1324–1339

Li Z, Yamauchi Y, Kamakura M, Murayama T, Goshima F, Kimura H & Nishiyama Y (2012) Herpes simplex virus requires poly(ADP-ribose) polymerase activity for efficient replication and induces extracellular signal-related kinase-dependent phosphorylation and ICP0-dependent nuclear localization of tankyrase 1. *J. Virol.* **86:** 492–503

Lu J, Ma Z, Hsieh J-C, Fan C-W, Chen B, Longgood JC, Williams NS, Amatruda JF, Lum L & Chen C (2009) Structure-activity relationship studies of small-molecule inhibitors of Wnt response. *Bioorg. Med. Chem. Lett.* **19:** 3825–3827

Lyons RJ, Deane R, Lynch DK, Ye ZS, Sanderson GM, Eyre HJ, Sutherland GR & Daly RJ (2001) Identification of a novel human tankyrase through its interaction with the adaptor protein Grb14. *J. Biol. Chem.* **276:** 17172–17180

MacDonald BT, Tamai K & He X (2009) Wnt/beta-catenin signaling: components, mechanisms, and diseases. *Dev. Cell* **17:** 9–26

Malanga M & Althaus FR (2005) The role of poly(ADP-ribose) in the DNA damage signaling network. *Biochem. Cell Biol. Biochim. Biol. Cell.* **83:** 354–364

Manke IA, Lowery DM, Nguyen A & Yaffe MB (2003) BRCT repeats as phosphopeptide-binding modules involved in protein targeting. *Science* **302:** 636–639

McCabe N, Cerone MA, Ohishi T, Seimiya H, Lord CJ & Ashworth A (2009) Targeting Tankyrase 1 as a therapeutic strategy for BRCA-associated cancer. *Oncogene* **28:** 1465–1470

McCutchen-Maloney SL, Matsuda K, Shimbara N, Binns DD, Tanaka K, Slaughter CA & DeMartino GN (2000) cDNA cloning, expression, and functional characterization of PI31, a proline-rich inhibitor of the proteasome. *J. Biol. Chem.* **275:** 18557–18565

Menear KA, Adcock C, Boulter R, Cockcroft X, Copsey L, Cranston A, Dillon KJ, Drzewiecki J, Garman S, Gomez S, Javaid H, Kerrigan F,

Knights C, Lau A, Loh VM Jr, Matthews ITW, Moore S, O'Connor MJ, Smith GCM & Martin NMB (2008) 4-[3-(4-cyclopropanecarbonylpiperazine-1-carbonyl)-4-fluorobenzyl]-2H-phthalazin-1-one: a novel bioavailable inhibitor of poly(ADP-ribose) polymerase-1. *J. Med. Chem.* **51:** 6581–6591

Middleton E Jr, Kandaswami C & Theoharides TC (2000) The effects of plant flavonoids on mammalian cells: implications for inflammation, heart disease, and cancer. *Pharmacol. Rev.* **52:** 673–751

Miwa M, Ishihara M, Takishima S, Takasuka N, Maeda M, Yamaizumi Z, Sugimura T, Yokoyama S & Miyazawa T (1981) The branching and linear portions of poly(adenosine diphosphate ribose) have the same alpha(1 leads to 2) ribose-ribose linkage. *J. Biol. Chem.* **256:** 2916–2921

Morrone S, Cheng Z, Moon RT, Cong F & Xu W (2012) Crystal structure of a Tankyrase-Axin complex and its implications for Axin turnover and Tankyrase substrate recruitment. *Proc. Natl. Acad. Sci. U. S. A.* **109:** 1500–1505

Murshudov GN, Skubák P, Lebedev AA, Pannu NS, Steiner RA, Nicholls RA, Winn MD, Long F & Vagin AA (2011) REFMAC5 for the refinement of macromolecular crystal structures. *Acta Crystallogr. D Biol. Crystallogr.* **67:** 355–367

Narwal M, Fallarero A, Vuorela P & Lehtiö L (2012a) Homogeneous Screening Assay for Human Tankyrase. *J. Biomol. Screen.* **17:** 593–604

Narwal M, Haikarainen T, Fallarero A, Vuorela PM & Lehtiö L (2013a) Screening and structural analysis of flavones inhibiting tankyrases. *J. Med. Chem.* **56:** 3507–3517

Narwal M, Koivunen J, Haikarainen T, Obaji E, Legala OE, Venkannagari H, Joensuu P, Pihlajaniemi T & Lehtiö L (2013b) Discovery of Tankyrase Inhibiting Flavones with Increased Potency and Isoenzyme Selectivity. *J. Med. Chem.* **56:** 7880–7889

Narwal M, Venkannagari H & Lehtiö L (2012b) Structural basis of selective inhibition of human tankyrases. *J. Med. Chem.* **55:** 1360–1367

Nottbohm AC, Dothager RS, Putt KS, Hoyt MT & Hergenrother PJ (2007) A colorimetric substrate for poly(ADP-ribose) polymerase-1, VPARP, and tankyrase-1. *Angew. Chem. Int. Ed Engl.* **46:** 2066–2069

Oka S, Kato J & Moss J (2006) Identification and characterization of a mammalian 39-kDa poly(ADP-ribose) glycohydrolase. *J. Biol. Chem.* **281:** 705–713

Oliver AW, Amé J-C, Roe SM, Good V, de Murcia G & Pearl LH (2004) Crystal structure of the catalytic fragment of murine poly(ADP-ribose) polymerase-2. *Nucleic Acids Res.* **32:** 456–464

Ono T, Kasamatsu A, Oka S & Moss J (2006) The 39-kDa poly(ADP-ribose) glycohydrolase ARH3 hydrolyzes O-acetyl-ADP-ribose, a product of the Sir2 family of acetyl-histone deacetylases. *Proc. Natl. Acad. Sci. U. S. A.* **103:** 16687–16691

Otto H, Reche PA, Bazan F, Dittmar K, Haag F & Koch-Nolte F (2005) In silico characterization of the family of PARP-like poly(ADP-ribosyl)transferases (pARTs). *BMC Genomics* **6:** 139

Ozaki Y, Matsui H, Asou H, Nagamachi A, Aki D, Honda H, Yasunaga S, Takihara Y, Yamamoto T, Izumi S, Ohsugi M & Inaba T (2012) Poly-ADP ribosylation of Miki by tankyrase-1 promotes centrosome maturation. *Mol. Cell* **47:** 694–706

Pacher P, Liaudet L, Soriano FG, Mabley JG, Szabó E & Szabó C (2002) The role of poly(ADP-ribose) polymerase activation in the development of myocardial and endothelial dysfunction in diabetes. *Diabetes* **51:** 514–521

Palm W & de Lange T (2008) How shelterin protects mammalian telomeres. *Annu. Rev. Genet.* **42:** 301–334

Pion E, Bombarda E, Stiegler P, Ullmann GM, Mély Y, de Murcia G & Gérard D (2003) Poly(ADP-ribose) polymerase-1 dimerizes at a 5' recessed DNA end in vitro: a fluorescence study. *Biochemistry (Mosc.)* **42:** 12409–12417

Polakis P (2000) Wnt signaling and cancer. *Genes Dev.* **14:** 1837–1851

Polakis P (2007) The many ways of Wnt in cancer. *Curr. Opin. Genet. Dev.* **17:** 45–51

Purnell MR & Whish WJ (1980) Novel inhibitors of poly(ADP-ribose) synthetase. *Biochem. J.* **185:** 775–777

Putt KS & Hergenrother PJ (2004) An enzymatic assay for poly(ADP-ribose) polymerase-1 (PARP-1) via the chemical quantitation of NAD(+): application to the high-throughput screening of small molecules as potential inhibitors. *Anal. Biochem.* **326:** 78–86

Pyriochou A, Olah G, Deitch EA, Szabó C & Papapetropoulos A (2008) Inhibition of angiogenesis by the poly(ADP-ribose) polymerase inhibitor PJ-34. *Int. J. Mol. Med.* **22:** 113–118

Rippmann JF, Damm K & Schnapp A (2002) Functional characterization of the poly(ADP-ribose) polymerase activity of tankyrase 1, a potential regulator of telomere length. *J. Mol. Biol.* **323:** 217–224

Rossmann MG, Moras D & Olsen KW (1974) Chemical and biological evolution of nucleotide-binding protein. *Nature* **250:** 194–199

De Rycker M & Price CM (2004) Tankyrase polymerization is controlled by its sterile alpha motif and poly(ADP-ribose) polymerase domains. *Mol. Cell. Biol.* **24:** 9802–9812

De Rycker M, Venkatesan RN, Wei C & Price CM (2003) Vertebrate tankyrase domain structure and sterile alpha motif (SAM)-mediated multimerization. *Biochem. J.* **372:** 87–96

Sbodio JI & Chi N-W (2002) Identification of a tankyrase-binding motif shared by IRAP, TAB182, and human TRF1 but not mouse TRF1. NuMA contains this RXXPDG motif and is a novel tankyrase partner. *J. Biol. Chem.* **277:** 31887–31892

Sbodio JI, Lodish HF & Chi N-W (2002) Tankyrase-2 oligomerizes with tankyrase-1 and binds to both TRF1 (telomere-repeat-binding factor 1) and IRAP (insulin-responsive aminopeptidase). *Biochem. J.* **361:** 451–459

Scherag A, Dina C, Hinney A, Vatin V, Scherag S, Vogel CIG, Müller TD, Grallert H, Wichmann H-E, Balkau B, Heude B, Jarvelin M-R, Hartikainen A-L, Levy-Marchal C, Weill J, Delplanque J, Körner A, Kiess W, Kovacs P, Rayner NW, et al (2010) Two new Loci for body-weight regulation identified in a joint analysis of genome-wide association studies for early-onset extreme obesity in French and german study groups. *PLoS Genet.* **6:** e1000916

Schraufstatter IU, Hyslop PA, Hinshaw DB, Spragg RG, Sklar LA & Cochrane CG (1986) Hydrogen peroxide-induced injury of cells and its prevention by inhibitors of poly(ADP-ribose) polymerase. *Proc. Natl. Acad. Sci. U. S. A.* **83:** 4908–4912

Schreiber V, Dantzer F, Ame J-C & de Murcia G (2006) Poly(ADP-ribose): novel functions for an old molecule. *Nat. Rev. Mol. Cell Biol.* **7:** 517–528

Scovassi AI (2004) Mitochondrial poly(ADP-ribosylation): from old data to new perspectives. *FASEB J. Off. Publ. Fed. Am. Soc. Exp. Biol.* **18:** 1487–1488

Seimiya H (2006) The telomeric PARP, tankyrases, as targets for cancer therapy. *Br. J. Cancer* **94:** 341–345

Seimiya H, Muramatsu Y, Ohishi T & Tsuruo T (2005) Tankyrase 1 as a target for telomere-directed molecular cancer therapeutics. *Cancer Cell* **7:** 25–37

Seimiya H, Muramatsu Y, Smith S & Tsuruo T (2004) Functional subdomain in the ankyrin domain of tankyrase 1 required for poly(ADP-ribosyl)ation of TRF1 and telomere elongation. *Mol. Cell. Biol.* **24:** 1944–1955

Seimiya H & Smith S (2002) The telomeric poly(ADP-ribose) polymerase, tankyrase 1, contains multiple binding sites for telomeric repeat binding factor 1 (TRF1) and a novel acceptor, 182-kDa tankyrase-binding protein (TAB182). *J. Biol. Chem.* **277:** 14116–14126

Sharifi R, Morra R, Appel CD, Tallis M, Chioza B, Jankevicius G, Simpson MA, Matic I, Ozkan E, Golia B, Schellenberg MJ, Weston R, Williams JG, Rossi MN, Galehdari H, Krahn J, Wan A, Trembath RC, Crosby AH, Ahel D, et al (2013) Deficiency of terminal ADP-ribose protein glycohydrolase

TARG1/C6orf130 in neurodegenerative disease. *EMBO J.* **32:** 1225–1237

Shay JW & Bacchetti S (1997) A survey of telomerase activity in human cancer. *Eur. J. Cancer Oxf. Engl. 1990* **33:** 787–791

Shebzukhov YV, Lavrik IN, Karbach J, Khlgatian SV, Koroleva EP, Belousov PV, Kashkin KN, Knuth A, Jager E, Chi N-W, Kuprash DV & Nedospasov SA (2008) Human tankyrases are aberrantly expressed in colon tumors and contain multiple epitopes that induce humoral and cellular immune responses in cancer patients. *Cancer Immunol. Immunother. CII* **57:** 871–881

Shervington A, Patel R, Lu C, Cruickshanks N, Lea R, Roberts G, Dawson T & Shervington L (2007) Telomerase subunits expression variation between biopsy samples and cell lines derived from malignant glioma. *Brain Res.* **1134:** 45–52

Shultz MD, Cheung AK, Kirby CA, Firestone B, Fan J, Chen CH-T, Chen Z, Chin DN, Dipietro L, Fazal A, Feng Y, Fortin PD, Gould T, Lagu B, Lei H, Lenoir F, Majumdar D, Ochala E, Palermo MG, Pham L, et al (2013a) Identification of NVP-TNKS656: The Use of Structure-Efficiency Relationships To Generate a Highly Potent, Selective, and Orally Active Tankyrase Inhibitor. *J. Med. Chem.* **56:** 6495–6511

Shultz MD, Kirby CA, Stams T, Chin DN, Blank J, Charlat O, Cheng H, Cheung A, Cong F, Feng Y, Fortin PD, Hood T, Tyagi V, Xu M, Zhang B & Shao W (2012) [1,2,4]triazol-3-ylsulfanylmethyl)-3-phenyl-[1,2,4]oxadiazoles: antagonists of the Wnt pathway that inhibit tankyrases 1 and 2 via novel adenosine pocket binding. *J. Med. Chem.* **55:** 1127–1136

Shultz MD, Majumdar D, Chin DN, Fortin PD, Feng Y, Gould T, Kirby CA, Stams T, Waters NJ & Shao W (2013b) Structure-Efficiency Relationship of [1,2,4]Triazol-3-ylamines as Novel Nicotinamide Isosteres that Inhibit Tankyrases. *J. Med. Chem.* **56:** 7049–7059

Siva AC, Raval-Fernandes S, Stephen AG, LaFemina MJ, Scheper RJ, Kickhoefer VA & Rome LH (2001) Up-regulation of vaults may be necessary but not sufficient for multidrug resistance. *Int. J. Cancer J. Int. Cancer* **92:** 195–202

Slade D, Dunstan MS, Barkauskaite E, Weston R, Lafite P, Dixon N, Ahel M, Leys D & Ahel I (2011) The structure and catalytic mechanism of a poly(ADP-ribose) glycohydrolase. *Nature* **477:** 616–620

Smith S, Giriat I, Schmitt A & de Lange T (1998) Tankyrase, a poly(ADP-ribose) polymerase at human telomeres. *Science* **282:** 1484–1487

Smith S & de Lange T (2000) Tankyrase promotes telomere elongation in human cells. *Curr. Biol. CB* **10:** 1299–1302

Szabó C, Cuzzocrea S, Zingarelli B, O'Connor M & Salzman AL (1997) Endothelial dysfunction in a rat model of endotoxic shock. Importance of the activation of poly (ADP-ribose) synthetase by peroxynitrite. *J. Clin. Invest.* **100:** 723–735

Tang B, Wang J, Fang J, Jiang B, Zhang M, Wang Y & Yang Z (2012) Expression of TNKS1 is correlated with pathologic grade and Wnt/β-catenin pathway in human astrocytomas. *J. Clin. Neurosci. Off. J. Neurosurg. Soc. Australas.* **19:** 139–143

Tao Z, Gao P, Hoffman DW & Liu H-W (2008) Domain C of human poly(ADP-ribose) polymerase-1 is important for enzyme activity and contains a novel zinc-ribbon motif. *Biochemistry (Mosc.)* **47:** 5804–5813

Tao Z, Gao P & Liu H (2009) Identification of the ADP-ribosylation sites in the PARP-1 automodification domain: analysis and implications. *J. Am. Chem. Soc.* **131:** 14258–14260

Thomas HD, Calabrese CR, Batey MA, Canan S, Hostomsky Z, Kyle S, Maegley KA, Newell DR, Skalitzky D, Wang L-Z, Webber SE & Curtin NJ (2007) Preclinical selection of a novel poly(ADP-ribose) polymerase inhibitor for clinical trial. *Mol. Cancer Ther.* **6:** 945–956

Vagin A & Teplyakov A (2010) Molecular replacement with MOLREP. *Acta Crystallogr. D Biol. Crystallogr.* **66:** 22–25

Venkannagari H, Fallarero A, Feijs KLH, Lüscher B & Lehtiö L (2013) Activity-based assay for human mono-ADP-ribosyltransferases

ARTD7/PARP15 and ARTD10/PARP10 aimed at screening and profiling inhibitors. *Eur. J. Pharm. Sci. Off. J. Eur. Fed. Pharm. Sci.* **49:** 148–156

Voronkov A, Holsworth DD, Waaler J, Wilson SR, Ekblad B, Perdreau-Dahl H, Dinh H, Drewes G, Hopf C, Morth JP & Krauss S (2013) Structural basis and SAR for G007-LK, a lead stage 1,2,4-triazole based specific tankyrase 1/2 inhibitor. *J. Med. Chem.* **56:** 3012–3023

Waaler J, Machon O, von Kries JP, Wilson SR, Lundenes E, Wedlich D, Gradl D, Paulsen JE, Machonova O, Dembinski JL, Dinh H & Krauss S (2011) Novel synthetic antagonists of canonical Wnt signaling inhibit colorectal cancer cell growth. *Cancer Res.* **71:** 197–205

Waaler J, Machon O, Tumova L, Dinh H, Korinek V, Wilson SR, Paulsen JE, Pedersen NM, Eide TJ, Machonova O, Gradl D, Voronkov A, von Kries JP & Krauss S (2012) A novel tankyrase inhibitor decreases canonical Wnt signaling in colon carcinoma cells and reduces tumor growth in conditional APC mutant mice. *Cancer Res.* **72:** 2822–2832

Wahlberg E, Karlberg T, Kouznetsova E, Markova N, Macchiarulo A, Thorsell A-G, Pol E, Frostell Å, Ekblad T, Öncü D, Kull B, Robertson GM, Pellicciari R, Schüler H & Weigelt J (2012) Family-wide chemical profiling and structural analysis of PARP and tankyrase inhibitors. *Nat. Biotechnol.* **30:** 283–288

Walley AJ, Asher JE & Froguel P (2009) The genetic contribution to non-syndromic human obesity. *Nat. Rev. Genet.* **10:** 431–442

Waring MJ (2010) Lipophilicity in drug discovery. *Expert Opin. Drug Discov.* **5:** 235–248

Wittes RE & Goldin A (1986) Unresolved issues in combination chemotherapy. *Cancer Treat. Rep.* **70:** 105–125

Yang CS, Landau JM, Huang MT & Newmark HL (2001) Inhibition of carcinogenesis by dietary polyphenolic compounds. *Annu. Rev. Nutr.* **21:** 381–406

Yang Y-G, Cortes U, Patnaik S, Jasin M & Wang Z-Q (2004) Ablation of PARP-1 does not interfere with the repair of DNA double-strand breaks, but compromises the reactivation of stalled replication forks. *Oncogene* **23:** 3872–3882

Yashiroda Y, Okamoto R, Hatsugai K, Takemoto Y, Goshima N, Saito T, Hamamoto M, Sugimoto Y, Osada H, Seimiya H & Yoshida M (2010) A novel yeast cell-based screen identifies flavone as a tankyrase inhibitor. *Biochem. Biophys. Res. Commun.* **394:** 569–573

Yeh T-YJ, Beiswenger KK, Li P, Bolin KE, Lee RM, Tsao T-S, Murphy AN, Hevener AL & Chi N-W (2009) Hypermetabolism, hyperphagia, and reduced adiposity in tankyrase-deficient mice. *Diabetes* **58:** 2476–2485

Yeh T-YJ, Meyer TN, Schwesinger C, Tsun Z-Y, Lee RM & Chi N-W (2006a) Tankyrase recruitment to the lateral membrane in polarized epithelial cells: regulation by cell-cell contact and protein poly(ADP-ribosyl)ation. *Biochem. J.* **399:** 415–425

Yeh T-YJ, Sbodio JI & Chi N-W (2006b) Mitotic phosphorylation of tankyrase, a PARP that promotes spindle assembly, by GSK3. *Biochem. Biophys. Res. Commun.* **350:** 574–579

Yeh T-YJ, Sbodio JI, Tsun Z-Y, Luo B & Chi N-W (2007) Insulin-stimulated exocytosis of GLUT4 is enhanced by IRAP and its partner tankyrase. *Biochem. J.* **402:** 279–290

Yélamos J, Schreiber V & Dantzer F (2008) Toward specific functions of poly(ADP-ribose) polymerase-2. *Trends Mol. Med.* **14:** 169–178

Zhang J & Snyder SH (1993) Purification of a nitric oxide-stimulated ADP-ribosylated protein using biotinylated beta-nicotinamide adenine dinucleotide. *Biochemistry (Mosc.)* **32:** 2228–2233

Zhang J-H, Chung TDY & Oldenburg KR (1999) A Simple Statistical Parameter for Use in Evaluation and Validation of High Throughput Screening Assays. *J. Biomol. Screen. Off. J. Soc. Biomol. Screen.* **4:** 67–73

Zhang Y, Liu S, Mickanin C, Feng Y, Charlat O, Michaud GA, Schirle M, Shi X, Hild M, Bauer A, Myer VE, Finan PM, Porter JA, Huang S-MA & Cong F (2011) RNF146 is a

poly(ADP-ribose)-directed E3 ligase that regulates axin degradation and Wnt signalling. *Nat. Cell Biol.* **13:** 623–629

Zhao F, Vermeer B, Lehmann U, Kreipe H, Manns MP, Korangy F & Greten TF (2009) Identification of a novel murine pancreatic tumour antigen, which elicits antibody responses in patients with pancreatic carcinoma. *Immunology* **128:** 134–140

Zingarelli B, Salzman AL & Szabó C (1998) Genetic disruption of poly (ADP-ribose) synthetase inhibits the expression of P-selectin and intercellular adhesion molecule-1 in myocardial ischemia/reperfusion injury. *Circ. Res.* **83:** 85–94